

https://dspace.org/

Cranial morphology and phylogenetic analysis of Cynosaurus suppostus (Therapsida, Cynodontia) from the upper Permian of the Karoo Basin, South Africa

van den Brandt, Marc; Abdala, Fernando

2018-03
Evolutionary Studies Institute
https://hdl.handle.net/10539/24254

Downloaded from a DSpace repository. https://dspace.org/

Cranial morphology and phylogenetic analysis of *Cynosaurus suppostus* (Therapsida, Cynodontia) from the upper Permian of the Karoo Basin, South Africa

Marc J. Van den Brandt[1*] & Fernando Abdala[1,2]

[1]*Evolutionary Studies Institute and School of Geosciences, University of the Witwatersrand, Johannesburg, WITS 2050, South Africa*

[2]*Unidad Ejecutora Lillo, CONICET-Fundación Miguel Lillo, Miguel Lillo 251, Tucumán, Argentina*

Received 29 November 2017. Accepted 16 March 2018

Non-mammaliaform cynodonts are an important fossil lineage which include the ancestors of mammals and which illustrate the gradual evolution of mammalian characteristics. The earliest cynodonts ('basal cynodonts') are known from the late Permian. *Cynosaurus suppostus* is the second most abundant basal cynodont from the late Permian of the Karoo Basin of South Africa, but is poorly studied, with the most recent description of this taxon being 50 years old. Since then, several important new specimens of this species have been collected, meriting a thorough description of its cranial anatomy and exploration of its interspecific variation. Here we present a comprehensive description of the cranial morphology of *Cynosaurus suppostus*, producing an updated diagnosis for the species and comparisons amongst basal cynodonts. *Cynosaurus* is identified by three autapomorphies amongst basal cynodonts: a subvertical mentum on the anterior lower jaw; a robust mandible with a relatively high horizontal ramus; and the broadest snout across the canine region, representing up to 31.74% of basal skull length. One of the new specimens described here preserves orbital scleral ossicles, structures rarely preserved in non-mammaliaform cynodonts. *Cynosaurus* is now only the third cynodont in which scleral ossicles have been reported. An updated phylogenetic analysis of basal cynodont interrelationships recovered *Cynosaurus suppostus* as a member of the Galesauridae in only two of 16 most parsimonious trees, providing poor support for its inclusion in that family. The majority of known *Cynosaurus* specimens were collected in a geographically restricted area approximately 150 kilometres in diameter. Most specimens have been recovered from the latest Permian *Daptocephalus* Assemblage Zone, with only two specimens known from the older *Cistecephalus* Assemblage Zone.

Keywords: Cynodontia, late Permian, Karoo Basin, South Africa.

Palaeontologia africana 2018. ©2018 Marc J. Van den Brandt & Fernando Abdala. This is an open-access article published under the Creative Commons Attribution 4.0 Unported License (CC BY4.0). To view a copy of the license, please visit http://creativecommons.org/licenses/by/4.0/. This license permits unrestricted use, distribution, and reproduction in any medium, provided the original author and source are credited.
The article is permanently archived at: https://hdl.handle.net/10539/24254 — Supplementary information is available for download at the same handle.

INTRODUCTION

Non-mammaliaform cynodonts include the ancestors of mammals and illustrate the gradual evolution of mammalian characteristics. Thus, they are essential for understanding the origins and evolution of typical mammalian morphology (Kemp 2005; Liu & Olsen 2010). The earliest or most basal cynodonts (non-eucynodonts) are known from the late Permian and Early Triassic, and consist mostly of small- to medium-sized carnivores and insectivores (Brink 1965; Kemp 1979, 2005, 2012; Botha *et al.* 2007; Botha-Brink & Abdala 2008; Kammerer 2016). They demonstrate early phases in the attainment of typical mammalian characteristics, such as complex multicusped postcanine teeth, double occipital condyles, and the initial development of a bony secondary palate (Sidor & Smith 2004).

Historically species-poor, the number of basal cynodonts known from the late Permian of South Africa has recently expanded, with the discovery of the oldest known cynodonts *Charassognathus* and *Abdalodon* from the *Tropidostoma* Assemblage Zone (AZ) (Botha *et al.* 2007; Kammerer 2016). In addition to these earliest forms, Permian cynodonts in the Karoo are represented by the abundant taxa *Procynosuchus* and *Cynosaurus* (Abdala & Ribeiro 2010, Viglietti *et al.* 2015: supplementary file) and the rare, derived taxon *Nanictosaurus* (Van Heerden 1976, Van Heerden & Rubidge 1990). Finally, a new, currently unnamed taxon was recently recovered from levels close to the Permo-Triassic boundary (Abdala & Smith 2011).

None of the late Permian species of cynodonts are known to have crossed the Permo-Triassic boundary (Botha-Brink & Abdala 2008), but the clade as a whole survived the extinction and radiated extensively in the Triassic. Early Triassic cynodonts from South Africa are represented by four basal taxa, *Progalesaurus*, *Galesaurus*, *Thrinaxodon* and *Platycraniellus* (Abdala 2007; Jasinoski *et al.* 2015; Jasinoski & Abdala 2017; Sidor & Smith 2004). Later Triassic cynodonts consist almost exclusively of the major clade Eucynodontia, with the exception of the relictual Middle Triassic basal cynodont *Bolotridon* (Abdala *et al*. 2005)

*Author for correspondence. E-mail: marcvandenbrandt@gmail.com

***Palaeontologia africana* 52: 201–221 — ISSN 2410-4418 [Palaeontol. afr.] Online only**
Permanently archived on the 27th of March 2018 at the University of the Witwatersrand, Johannesburg, South Africa.
The article is permanently archived at: https://hdl.handle.net/10539/24254 — Supplementary information is available for download at the same handle.

Cynosaurus suppostus was initially described by Owen (1876; Fig.1A–B) as *Cynosuchus suppostus*, and a second species, *Cynosuchus whaitsi*, was established by Haughton (1918; Fig. 1C–D). Schmidt (1927) proposed the replacement name *Cynosaurus* for this genus, because the name *Cynosuchus* was preoccupied by a crocodilian (*Cynosuchus* Gray 1862). Broom (1931) reassigned *C. whaitsi* to a new genus (*Cynosuchoides*) and Brink (1965) described a second specimen (BP/1/3926) referred to *Cynosuchoides whaitsi*.

In their revised classification of cynodonts, Hopson & Kitching (1972) considered *Cynosuchoides whaitsi* to be synonymous with *Cynosuchus suppostus*. They also considered the type specimens of the nominal Permian cynodont taxa *Nanictosaurus kitchingi*, *Mygalesuchus peggyae* and *Baurocynodon gracilis* to be juvenile specimens of *Cynosaurus suppostus*, leaving it as the only valid species of *Cynosaurus*. However, Van Heerden (1976) and Van Heerden & Rubidge (1990) later argued against synonymization of *Nanictosaurus* with *Cynosaurus*, upholding *Nanictosaurus* as a valid, more derived taxon.

With the most recent anatomical description of *Cynosaurus* being over 50 years old (Brink 1965), this taxon is due for reevaluation. Even though *Cynosaurus* is the second most abundant late Permian cynodont, the cranial morphology of the species is still inadequately known, as recognized by Van Heerden (1976) and Van Heerden & Rubidge (1990). Furthermore, several informative, undescribed specimens of *Cynosaurus* are present in South African collections (AM4947, BP/1/1563, BP/1/4469, SAM-PK-K5211 and SAM-PK-K10694) (Fig. 2). Although too fragmentary to assign to *Cynosaurus* with certainty, additional potential specimens are also known which may bear on the distribution of this taxon (see Geographic and geological provenance and stratigraphic range).

The aim of this paper is to address the current lack of knowledge of *Cynosaurus suppostus* with a comprehensive description of its cranial morphology, incorporating all available specimens of the taxon. This new information is used to rescore character data for *Cynosaurus* in a recently published data matrix of basal cynodonts (Kammerer 2016) and to test the phylogenetic placement of this taxon in light of different proposals that include it inside (Sidor & Smith 2004) or outside (Abdala 2007; Kammerer 2016) of the otherwise-Triassic family Galesauridae.

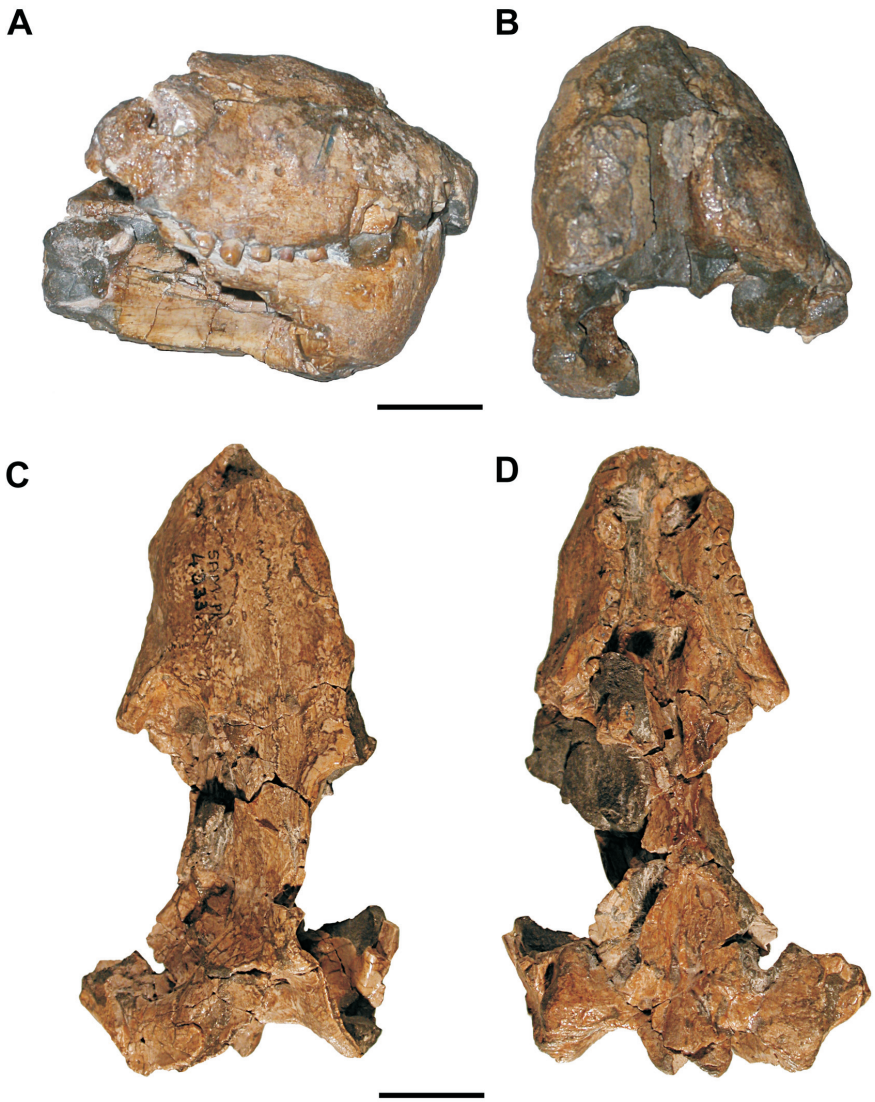


Figure 1. Holotypes of *Cynosaurus*. **A**–**B**, NHMUK PV R1718 *Cynosuchus suppostus* (Owen 1876) in (**A**) right lateral and (**B**) dorsal view; **C**–**D**, SAM-PK-4333 *Cynosaurus whaitsi*, (Haughton 1918) in (**C**) dorsal and (**D**) ventral view. Scale bar equals 20 mm.

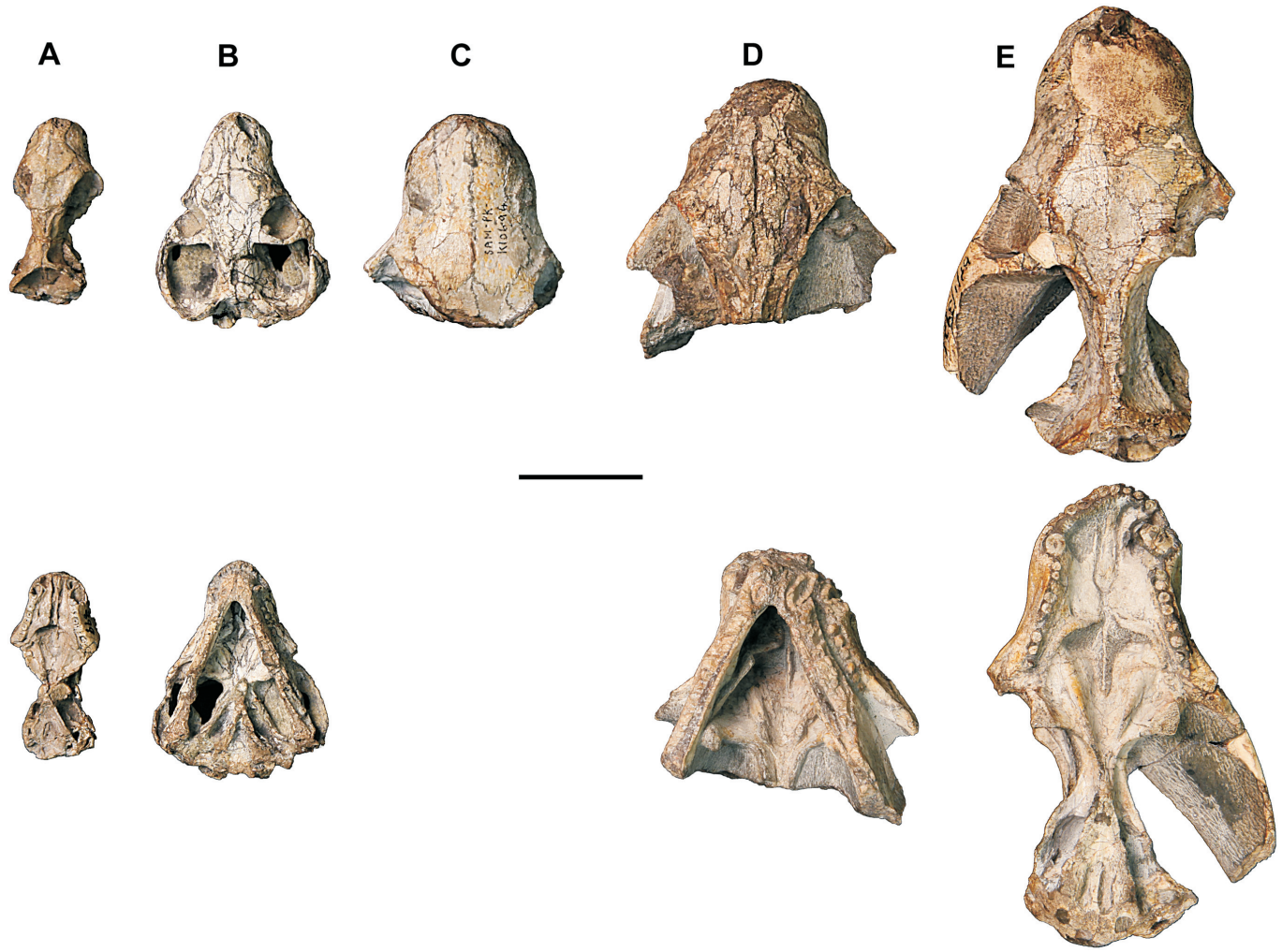


Figure 2. Newly described specimens (besides BP/1/3926) referred to *Cynosaurus suppostus* ordered in a growth series. **A**, BP/1/1563 in dorsal and ventral view; **B**, BP/1/4469 in dorsal and ventral view; **C**, SAM-PK-K10694 indorsal view; **D**, AM4947 in dorsal and ventral view; **E**, BP/1/3926 in dorsal and ventral view. Scale bar equals 30 mm.

MATERIAL AND METHODS

The following nine specimens of *Cynosaurus* and comparative specimens of other basal cynodonts were examined for this study:

Holotypes

NHMUK PV R1718, the holotype of *Cynosuchus suppostus* Owen (1876), poorly-preserved snout up to the orbits and partial mandible in occlusion (Fig. 1A–B).

SAM-PK-4333, the holotype of *Cynosuchus whaitsi* Haughton (1918), well-preserved cranium lacking lower jaw (Fig. 1C–D).

Referred material

AM4947, damaged partial cranium and mandible (Fig. 2D).

BP/1/1563, partial well-preserved small cranium, lacking lower jaw (Fig. 2A).

BP/1/3926, the second specimen of *C. whaitsi* described by Brink (1965), well-preserved cranium lacking lower jaw (Fig. 2E).

BP/1/4469, virtually complete and well-preserved small cranium including lower jaw (Fig. 2B).

SAM-PK-K5211, small partial skull.

SAM-PK-K5819, an unprepared partial snout exposing broken upper postcanines.

SAM-PK-K10694, very well-preserved anterior cranium and lower jaw (Fig. 2C).

Comparative material

Procynosuchus delaharpeae (BP/1/226, BP/1/591, BP/1/2600, BP/1/3748, NHMUK PV R 37054, RC 5, RC 12, RC 72, RC 87, RC 92, RC 130), *Galesaurus planiceps* (AMNH FARB 2223, AMNH FARB 2227, BP/1/5064, NMQR 860, NMQR 1451, NMQR 3340, NMQR 3542, SAM-PK-K9956), *Thrinaxodon liorhinus* (BP/1/1375, BPI/1/2513a, BP/1/4263, BP/1/4280, BP/1/4714, BP/1/5208, BP/1/5372, BSPG 1934 VIII 506, MMK 4283, NHMUK R511, NHMUK R3731, NHMUK R5480, NMQR 24, NMQR 812, NMQR 810, SAM-PK-K379, SAM-PK-K1467, SAM-PK-K1498, SAM-PK-K1499, TM 81, TM 180, UCMP 42865, UCMP 42866, UCMP 42877, UCMP 42878), *Progalesaurus lootsbergensis* (SAM-PK-K9954) and *Platycraniellus elegans* (TM 25) were consulted.

Specimens of *Cynosaurus* were CT-scanned at the Evolutionary Studies Institute (University of the Witwatersrand, Johannesburg, South Africa) using a Nikon Metrology XTH 225/320 LC dual source CT system. We

used these data to present a virtual reconstruction of the specimen BP/1/1563 (Fig. 9A–D). As this contribution is centred on the anatomical description of gross external morphology in *Cynosaurus*, we have not used the CT data to reconstruct endocranial morphology. Studies of internal cranial structure as well as of morphological changes in the snout of *Cynosaurus* over ontogeny will be addressed in future studies. However, CT data were used to reveal features hidden under matrix or occluded by bone (e.g. incisor number in the occluded lower jaw of BP/1/4469).

Key to interpretive drawings

Sutures in solid lines have been positively identified; those in dotted lines are extrapolated. Light grey indicates matrix, dark grey indicates plaster, sides of bones or bone breaks, black indicates foramen or fenestra.

SYSTEMATIC PALAEONTOLOGY

THERAPSIDA Broom, 1905
CYNODONTIA Owen, 1861
EPICYNODONTIA Hopson and Kitching, 2001
CYNOSAURUS Schmidt, 1927

Cynosaurus suppostus (Owen, 1876)

Synonyms

Cynosuchus suppostus Owen 1876; *Cynosuchus whaitsi* Haughton 1918 (=*Cynosuchoides whaitsi* Broom 1931).

Emended diagnosis

Medium-sized basal cynodont with three autapomorphies: subvertical mentum on the anterior lower jaw; a robust mandible with a relatively high horizontal ramus; broad snout (measured across the upper canines) representing up to 31.74% of basal skull length; adult lacking pineal foramen. Adult dental formula of I4/i3, C1/c1, PC 8-9/pc8-9. As in *Progalesaurus*, strong longitudinal grooves or striations present on the canines; as in *Galesaurus*, incomplete bony secondary palate with relatively narrow cleft between the maxilla and palatine processes posteriorly; as in *Thrinaxodon*, splenial continues posteriorly well beyond the level of the pterygoid processes; as in *Platycraniellus* and *Progalesaurus*, short snout representing as little as 32.25% of basal skull length; as in *Progalesaurus*, *Galesaurus* and adult *Thrinaxodon*, temporal ramus of the postorbital extends posteriorly in two directions, dorsally and ventrally, creating a forked shape; as in *Procynosuchus*, scleral ossicles present; as in *Progalesaurus*, *Galesaurus* and *Platycraniellus*, simple first and second postcanines, showing a main recurved cusp with a convex anterior edge and with a single posterior accessory cusp; more complex posterior postcanines with a main recurved cusp and both single anterior and posterior accessory cusps; postcanine teeth lack lingual cingula.

Geographic and geological provenance and stratigraphic range

Most *Cynosaurus* specimens were found within an area approximately 150 kilometres in diameter. Seven of the nine specimens were found within a restricted region between the towns of Graaff-Reinet, Murraysburg and Nieu Bethesda in the Eastern Cape and Western Cape provinces of South Africa (Table 1, Fig. 3). A similarly-restricted geographic distribution has also been reported in some other *Cistecephalus-Daptocephalus* AZ therapsids, such as the dicynodont *Pelanomodon* and the gorgonopsian *Clelandina* (Kammerer *et al.* 2015, Kammerer 2017). This region also includes areas known for producing Lower Triassic specimens of *Galesaurus*, *Progalesaurus* and *Thrinaxodon*, namely Lootsberg (Tweefontein, Lootsberg Pass and Old Wapadsberg Pass) and Nieu Bethesda (Ripplemead) (Sidor & Smith 2004; Jasinoski & Abdala 2017). The Permo-Triassic boundary is also exposed in this region (Smith & Botha-Brink 2014).

All known *Cynosaurus* specimens have been found in sedimentary beds corresponding to the *Cistecephalus* and *Daptocephalus* AZs, Balfour Formation, Beaufort Group, Karoo Supergroup, South Africa (upper Permian) (Table 1, Fig. 3). Viglietti *et al.* (2015: supplementary file) reported 11 specimens of *Cynosaurus*, three from the *Cistecephalus* AZ, five from the Lower *Daptocephalus* AZ and three from the Upper *Daptocephalus* AZ. Five of these 11 specimens cannot be confirmed as members of *Cynosaurus*. BP/1/47 (holotype of *Baurocynodon gracilis*, synonymized with *C. suppostus* by Hopson & Kitching 1972), BP/1/863 and BP/1/5741 are too fragmentary for confident identification as *Cynosaurus*. BP/1/4259 repre-

Table 1. *Cynosaurus suppostus* specimen location table showing the geographic distribution of the specimens. ECP = Eastern Cape Province, WCP = Western Cape Province.

Specimen	Specimen no.	District	Farm	Assemblage Zone
a	BP/1/1563	Murraysburg (WCP)	Ringsfontein	*Daptocephalus*
b	BP/1/4469	Graaff-Reinet (ECP)	Zwagershoek	*Daptocephalus*
c	SAM-PK-4333	Graaff-Reinet (ECP)	Weltevreden	*Daptocephalus*
d	BP/1/3926	New Bethesda (ECP)	Tweefontein	*Daptocephalus*
e	SAM-PK-K10694	Graaff-Reinet (ECP)	Krugerskraal	*Daptocephalus*
f	SAM-PK-K5211	Graaff-Reinet (ECP)	Graaff-Reinet Allotment Area	*Cistecephalus*
g	SAM-PK-K5819	Graaff-Reinet (ECP)	Doornplaats (Rust 126)	*Cistecephalus*
	NHMUK PV R1718	Graaff-Reinet (ECP)	Unknown	*Daptocephalus**
	AM4947	Unknown	Unknown	Unknown

*Sneeuwberg mountain range, Graaff-Reinet, Eastern Cape. Original locality unreliable. Suggested by Kitching (1977) as probably coming from levels corresponding to the *Daptocephalus* Assemblage Zone, as in most other known skulls of the genus *Cynosaurus*.

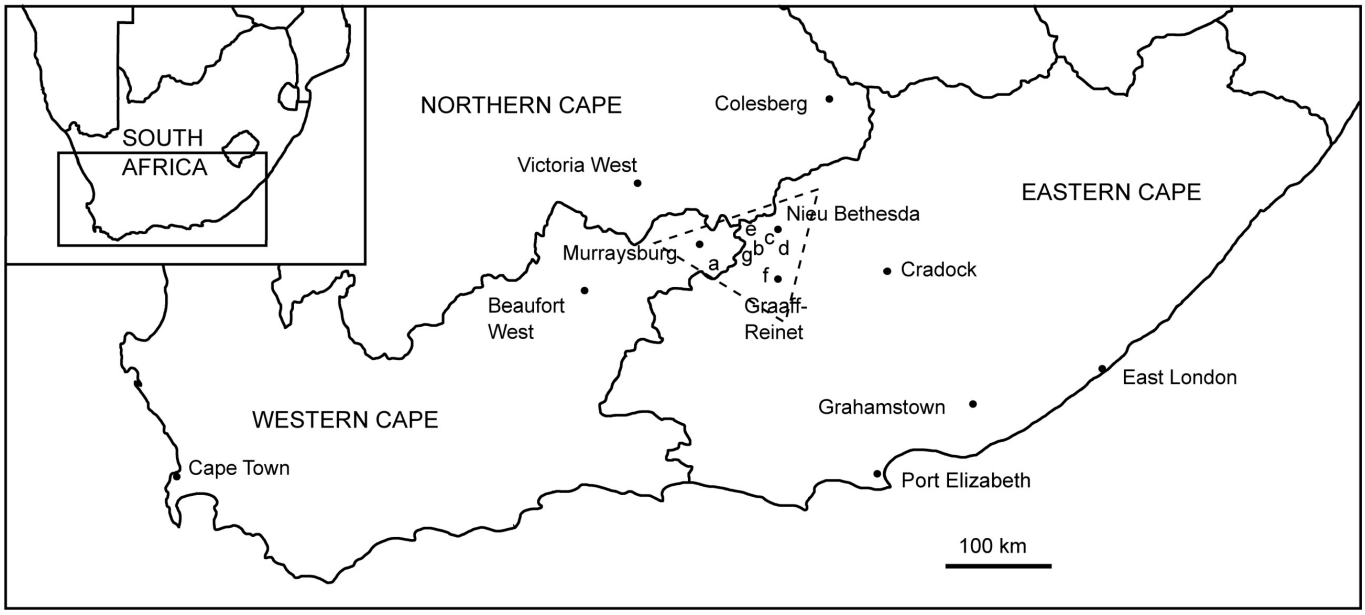


Figure 3. A map of South Africa, showing the geographic locations of *Cynosaurus* specimens found, all within the dotted triangle formed by the towns of Graaff-Reinet, Murraysburg and Nieu Bethesda. Letters denote localities of specimens: **a**, BP/1/1563; **b**, BP/1/4469; **c**, SAM-PK-4333; **d**, BP/1/3926; **e**, SAM-PK-K10694; **f**, SAM-PK-K5211; **g**, SAM-PK-K5819 (See Table 1).

sents a forelimb of the similarly-named gorgonopsian *Cyonosaurus*, not *Cynosaurus*. BPI/1/4281 exhibits morphology of the intertemporal region, internal choana and basicranium that does not match that of *Cynosaurus*, and appears to represent a different cynodont taxon. Three specimens included in the current description (AM4947, NHMUK PV R1718 and SAM-PK-K10694) were not considered in the study of Viglietti *et al.* (2015). This leaves a total of nine confidently-identified specimens of *Cynosaurus* (Table 1, Fig. 3), five of which were previously unpublished (AM4947, BP/1/1563, BP/1/4469, SAM-PK-K5211 and SAM-PK-K10694). The geologically oldest specimen is represented by the fragmentary specimen SAM-PK-K5211 from the *Cistecephalus* AZ (Viglietti *et al.* 2015). Most representatives of *Cynosaurus* are known from the geologically younger *Daptocephalus* AZ. BP/1/5741, identified as the last appearance datum for *Cynosaurus* in the upper *Daptocepalus* AZ (Viglietti *et al.* 2015), is poorly preserved and its lower jaw does not appear to show the typical high chin of *Cynosaurus*, so we cannot endorse its identity as *Cynosaurus*. The species appears to be better represented in the Lower *Daptocephalus* Zone (where it makes up 1% of 477 tetrapod specimens), than in the Upper *Daptocephalus* Zone (2% of 151 tetrapod specimens) (Viglietti *et al.*, 2015: figure 4).

DESCRIPTION

Preservation

NHMUK PV R1718 comprises a snout with lower jaw, broken just anterior to the orbits. The postcanine crowns are broken off on both right and left sides (Fig. 1A–B).

SAM-PK-4333 comprises a dorso-ventrally and diagonally crushed skull lacking the lower jaw and with incomplete zygomas (Fig. 1C–D). The majority of the postcanines are broken off approximately halfway down the crown.

BP/1/1563 is a very small skull (basal skull length of 50.29 mm, Table 2) lacking the lower jaw (Fig. 2A). The majority of both zygomatic arches are not preserved, including the ventral and posterior margins of both orbits. The anteroventral portion of the premaxilla is damaged, lacking the incisors. The upper canines are not preserved, having only the upper canine alveoli. Postcanine tooth crowns are not preserved – the majority of the teeth are broken off at or shortly above the alveolar margin (Fig. 2A).

BP/1/4469 comprises a well-preserved skull with lower jaw, but has some damage to the left jugal, at the ventral orbital margin (Fig. 2B). Although the skull is covered by cracks, sutures are identifiable. The dentition is well preserved. Additional preparation of the palate and the temporal region was performed for this study.

SAM-PK-K10694 comprises a snout with lower jaw and has the upper and lower postcanines very well preserved (Fig. 2C). The lower incisors are not preserved, but their alveoli are. A vertebra is visible below the jaw. Additional preparation of the orbits was performed for this study.

AM4947 comprises a poorly-preserved and damaged cranial specimen, but with well-preserved upper postcanines (Fig. 2D). There is some damage to the left postcanine series. Additional preparation of the left suborbital region was performed for this study.

BP/1/3926 is damaged, with parts of the cranium having been infilled with plaster, notably the right anterior portion of the nasal and the orbital edge of the left jugal (Fig. 2E). The anterior sides of the right premaxilla below the naris and the left premaxilla above the naris are damaged, with the right incisors partially exposed and the left incisors broken off at their emergence. A large portion of the left posterior squamosal is missing. The right zygoma is not preserved. Tooth crowns are not preserved, with the majority of the teeth broken off at or shortly above the alveolar margin. Additional preparation of the basicranial

Table 2. Cranial measurements of *Cynosaurus suppostus* specimens, in mm.

No.	Measurement	SAM-PK-4333	SAM-PK-K10694	BP/1/3926	AM4947	BP/1/4469	BP/1/1563
1	Basal skull length (BSL)	121.69		115.26		56.31	50.29
2	Middle dorsal length	99.03		102.31		45.46	41.65
3	Snout length (SL)	45.93	33.56	44.42	35.13 (a)	21.85	16.22
4	Orbital length (OL)	22.88 (b)	16.45 (b)	20.51	21.05 (b)	10.15	9.68 (b)
5	Temporal length (TL)			37.38		13.46	15.75
6	Minimum interorbital width/distance	27.77	28.33	31.21	26.42	14.19	10.79
7	Orbital diameter	17.88 (b)	14.84 (b)	21.44	18.90 (b)	8.44	9.40 (b)
8	Secondary palate length			36.56	31.64 (e)	18.83	14.17
9	Width of snout at anterior margin of orbits	49.89	41.9	51.28	44.69	27.38	22.24
10	Upper canine width	28.06	28.74	35.08	27.84	16.07	14.98
11	Maximum width of snout over upper canines (SW)	29.29 (c)	30.42	36.58	29.28	17.41	14.98
12	Lower canine width		20.42		22.78		
13	Max width of snout under canines		21.84		28.67		
14	Lower postcanine series length		20.27				
15	Upper postcanine series length	24.19	21.72	27.25	23.72	11.66	14.03
16	Anterior upper post canine distance	18.19	18.04	20.67	20.02	10.55	8.70
17	Posterior upper post canine distance	26.25	35.68	33.94	30.47	15.99	16.66
18	Maximum width of skull (W)			87.96 (d)		44.37	
19	Maximum height of zygomatic arch	11.43		12.57		8.5	
20	Occipital plate height	39.1		40.15		17.02	14.20
21	Occipital plate base width	52.97		41.84		19.6	15.29
22	Basicranial girder width			11.24	8.01	6.7	6.14
23	Transverse process width	43.64		36.35	33.59	17.27	
24	Occipital condyle width	16.36				9.81	8.34
25	Proportion: SL/BSL	37.74%		38.54%		38.80%	32.25%
26	Proportion: W/BSL			76.31%		78.80%	
27	Proportion: SW/BSL	24.07%		31.74%		30.92%	29.79%
28	Proportion: OL/BSL	18.80%		17.79%		18.03%	19.25%
29	Proportion: TL/BSL			32.43%		23.90%	31.32%

Notes:
(a) Estimate, as anterior border of snout is damaged/missing.
(b) Estimate, posterior half of orbit is missing/broken off.
(c) Estimate, as cranium is distorted and crushed flat.
(d) Estimate, right zygomatic arch missing, so doubled left zygomatic arch measurement.
(e) Estimate, as anterior border of snout is damaged/missing.

region of this specimen was performed for this study.

SAM-PK-K5211 comprises a fragmentary skull lacking the anterior portion of the snout and lower jaw.

SAM-PK-K5819 comprises a partial snout exposing broken upper postcanines.

Cranial measurements and proportions

Basal skull length (BSL) varies between 50.29 mm to 121.69 mm (Table 2). The snout length (SL) is comparatively longer than the temporal length (TL) in both small and large specimens.

The snout length (SL) varies between 32.25% to 38.80% of the BSL (Table 2: row 25) with most of the large specimens close to the higher value.

The cranial width (W) is 76.31% to 78.80% of the BSL (Table 2: row 26) indicating a relatively wide skull for a basal cynodont, second only to *Platycraniellus* at 88% (Abdala 2007).

The snout width (SW) (measured above the upper canines) is very broad, at up to 31.74% of basal skull length (BSL) for the large and undistorted specimen BP/1/3926. All large *Cynosaurus* specimens are over 30% for this measure (Table 2: row 27).

The orbital length (OL) varies between 17% to 19% of the BSL (Table 2: row 28) whereas the temporal length (TL) varies between 32% (for the large specimen BP/1/3926) to 23% of the BSL (Table 2: row 29).

Snout

Premaxilla

The premaxilla is a small, elongated bone, located at the anterior margin of the snout, forming the anteromedial and ventral margins of the external naris. In SAM-PK-K10694 and BP/1/4469, the premaxilla is well preserved and includes the dorsal ascending process that extends dorsally onto the anterior nasal edge, then continues posteriorly 3–4 mm beyond the level of the posterior margin of the naris (Figs 4A, 4B, 8A). The dorsal ascending process of the premaxilla extends proportionally further posteriorly in the smaller specimen BP/1/4469 than the larger SAM-PK-K10694. In BP/1/3926, the premaxilla houses a small anterior premaxillary foramen above the first incisor. This foramen is also observed on the right side of BP/1/4469.

Septomaxilla

The septomaxilla is small and elongated and is well preserved in SAM-PK-K10694 and BP/1/4469.The septomaxilla in cynodonts can be divided into the body and the facial process (Sidor & Smith 2004). The body forms the inside border of each nasal passage, covering the floor of the external naris. In SAM-PK-K10694, the body of the septomaxilla preserves the horizontal, intranarial process, forming a flat bridge or shelf that divides each nasal

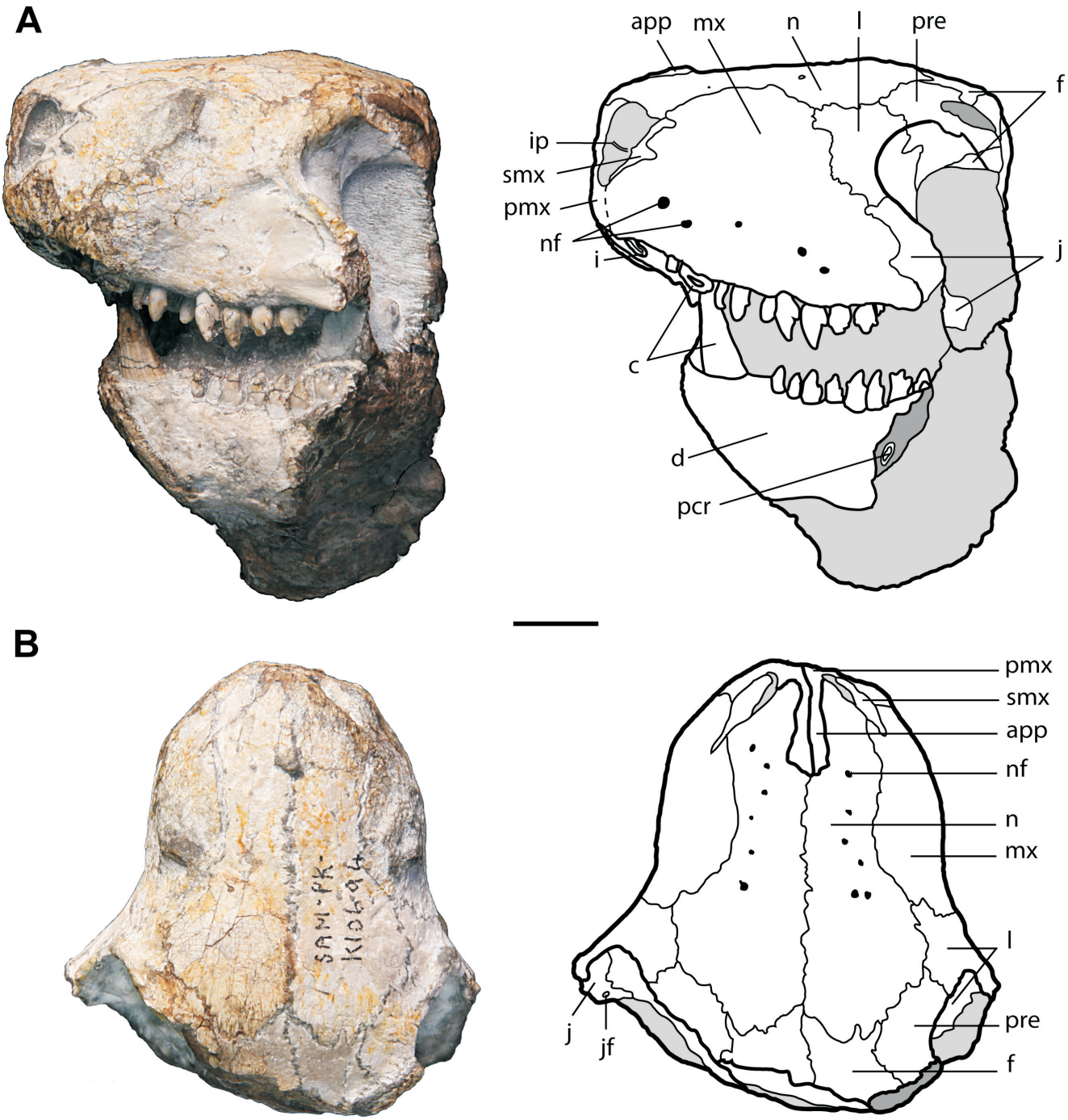


Figure 4. Photograph and interpretive drawing of *Cynosaurus suppostus*, specimen SAM-PK-K10694, **A**, left lateral view; **B**, dorsal view. Abbreviations: **app**, ascending process of the premaxilla; **c**, canine; **d**, dentary; **f**, frontal; **i**, incisor; **ip**, intranarial process; **j**, jugal; **jf**, jugal foramen; **l**, lacrimal; **mx**, maxilla; **n**, nasal; **nf**, nutritive foramina; **pcr**, postcanine root; **pmx**, premaxilla; **pre**, prefrontal; **smx**, septomaxilla. Scale bar equals 10 mm.

passage into two approximately equal upper and lower halves (Fig. 4A).

In SAM-PK-K10694 and BP/1/4469, the septomaxillary facial process covers the posterior margin of the external naris before forming a very short, thin laterally-located process between the maxilla and nasal (Figs 4A, 8A). There is no discernible septomaxillary foramen visible on the lateral surface of the snout.

Maxilla

The maxilla is a large bone that forms most of the lateral side of the snout. This bone is bounded by its anterior contact with the premaxilla and septomaxilla, its long dorsal contact with the nasal, its posterior contact with the lacrimal and the jugal, and its ventral alveolar border.

The lateral surface of the maxilla contains numerous small nutritive foramina, extending posteriorly from a region above the last incisor to the level of the fifth or sixth postcanine (Figs 4A, 6A, 8A, 9C). These foramina are laid out in two roughly horizontal parallel lines. The foramina in the ventral row are generally larger than those in the dorsal one. The ventral foramina row of SAM-PK-K10694 has a single, noticeably larger foramen in the anterior portion of the maxilla, anterior to the level of the canine (Fig. 4A).

In dorsal view, the maxilla is convex anteriorly, with a

ridge or swelling above each canine, whereas posteriorly the maxilla becomes concave just before contacting the lacrimal, and flares outwardly where it contacts the jugal below the orbit (Figs 1, 2, 5). In SAM-PK-K10694, the maxilla carries a raised rounded projection, near the dorsal contact with the nasal bones, probably related to the presence of the upper canine root (Fig. 4).

Nasal

The nasal is a large bone that covers the majority of the dorsal surface of the snout. Anteriorly, the nasal forms the dorsal edge of the external naris, between the septomaxilla and the ascending process of the premaxilla. The nasal bone is broader posteriorly than anteriorly, showing the greatest breadth where the bone contacts the lacrimal.

The external surface of the nasal in SAM-PK-K10694 contains numerous small nutritive foramina, arranged in an anteroposteriorly-oriented line or row, extending from near the anterior margin of the nasal to a point just beyond its narrowest concave region (Fig. 4B). The smaller specimens BP/1/4469 and BP/1/1563 also display these nasal nutritive foramen rows, but they are formed by fewer foramina than in the larger specimen (Fig. 9A). The naso-frontal suture is an inverted V-shape in most specimens (Fig. 4B), but is straighter in the large specimen BP/1/3926 (Fig. 5A).

Posteromedially, the nasal presents a slightly raised ridge near the contact with the frontal, as seen in BP/1/3926 and SAM-PK-K10694.

Orbito-temporal region

Frontal

The frontal bone is elongated anteroposteriorly and contacts the nasals anteriorly, the prefrontals anterolaterally and the postorbitals posterolaterally. The frontal does not form part of the dorsal margin of the orbits but reaches close to the orbital margin in the smaller specimen BP/1/4469.

In dorsal view, the frontal initially widens posteriorly, along the lateral contact with the prefrontal, and tapers posteriorly along the lateral contact with the postorbital and parietal (Figs 5A, 9A). The frontal contacts the parietal at the narrowest posterior point on the sagittal crest. In BP/1/3926, the frontal is slightly depressed compared to the level of the surrounding postorbital bone.

In lateral view, a small portion of the frontal appears below the prefrontal and postorbital as an elongated segment forming part of the dorsal margin of the orbital vacuity (Figs 4A, 6A).

Lacrimal

The lacrimal is a small bone forming the anterior edge of the orbit and contacts the prefrontal and the nasal dorsally, the maxilla anteriorly, and the jugal posteroventrally. On the anterior margin of the orbit of SAM-PK-K10694 and AM4947 there is a protuberance at the level of the lacrimal foramina. In SAM-PK-K10694 and BP/1/1563, two foramina are observed inside the anterior margin of the orbit, which are positioned vertically, approximately 3 mm apart. The ventral foramen is the larger. Although these two foramina appear to be present in BP/1/3926, damage and poor preservation makes confirmation difficult.

Prefrontal

The prefrontal is a small bone forming the anterodorsal edge of the orbit, contacting the frontal medially, the nasal anteriorly, the lacrimal anteroventrally and the postorbital posteriorly. The contact of the prefrontal with the frontal shows a longitudinal suture, directed slightly towards the lateral side posteriorly (Figs 4B, 5A, 9A). In SAM-PK-K10694 and BP/1/3926 the level of the postorbital is higher than the level of the prefrontal at the contact whereas in the smaller specimens these bones are at the same level.

Postorbital

The postorbital contacts the prefrontal anteriorly, the frontal dorsally, and the jugal ventrally. The postorbital forms: a) the dorsal margin of the orbit, contacting the prefrontal anteriorly, b) the posterodorsal portion of the postorbital bar, and c) the posterior temporal ramus of the postorbital, which covers the lateral surface of the parietal, ventral to the sagittal crest (Fig. 5A). In lateral view, the temporal ramus extends posteriorly in two directions, dorsally and ventrally, creating a forked shape, with the dorsal extension reaching below the orbito-temporal groove to contact the epipterygoid (Fig. 6A).

In BP/1/4469, the contact of the postorbital and the jugal in the postorbital bar displays a wedge shape (Fig. 8A), with the jugal overlapping the postorbital and creating an inverted V-shape at the contact. The jugal-postorbital contact occurs approximately midway along the postorbital bar.

Orbital scleral ossicles are preserved in the matrix of the left orbit of AM4947 (Fig. 7). These elements are located out of place in two parallel diagonal rows. Seven small scleral ossicles are visible in these rows, the upper row containing three and the lower row four bones. They are very delicate, laminar, and rectangular.

Jugal

The jugal forms the suborbital bar anteriorly, the ventral portion of the zygomatic arch posteriorly, and the ventral portion of the postorbital bar dorsally. This bone contacts the maxilla anteriorly, the lacrimal anterodorsally, the squamosal posteriorly and the postorbital dorsally.

In SAM-PK-K10694, the jugal extends anteriorly, as part of the suborbital bar, contacting the maxilla ventrally, and extending up to the level of the anterior margin of the orbit, where the bone contacts the lacrimal anteriorly (Fig. 4A). Within the left orbit, the jugal shows a single foramen (Fig. 4B). The suborbital bar does not show any process or angulation between the maxilla and the jugal.

Only BP/1/4469 preserves complete zygomatic arches, which are wide, robust and laterally flared (Fig. 8). The jugal makes up a large portion of the zygomatic arch, and extends posterolaterally outwards in a convex shape, accommodating the squamosal dorsally.

The inferior margin of the jugal in the zygomatic arch is longitudinally well developed and low. The temporal

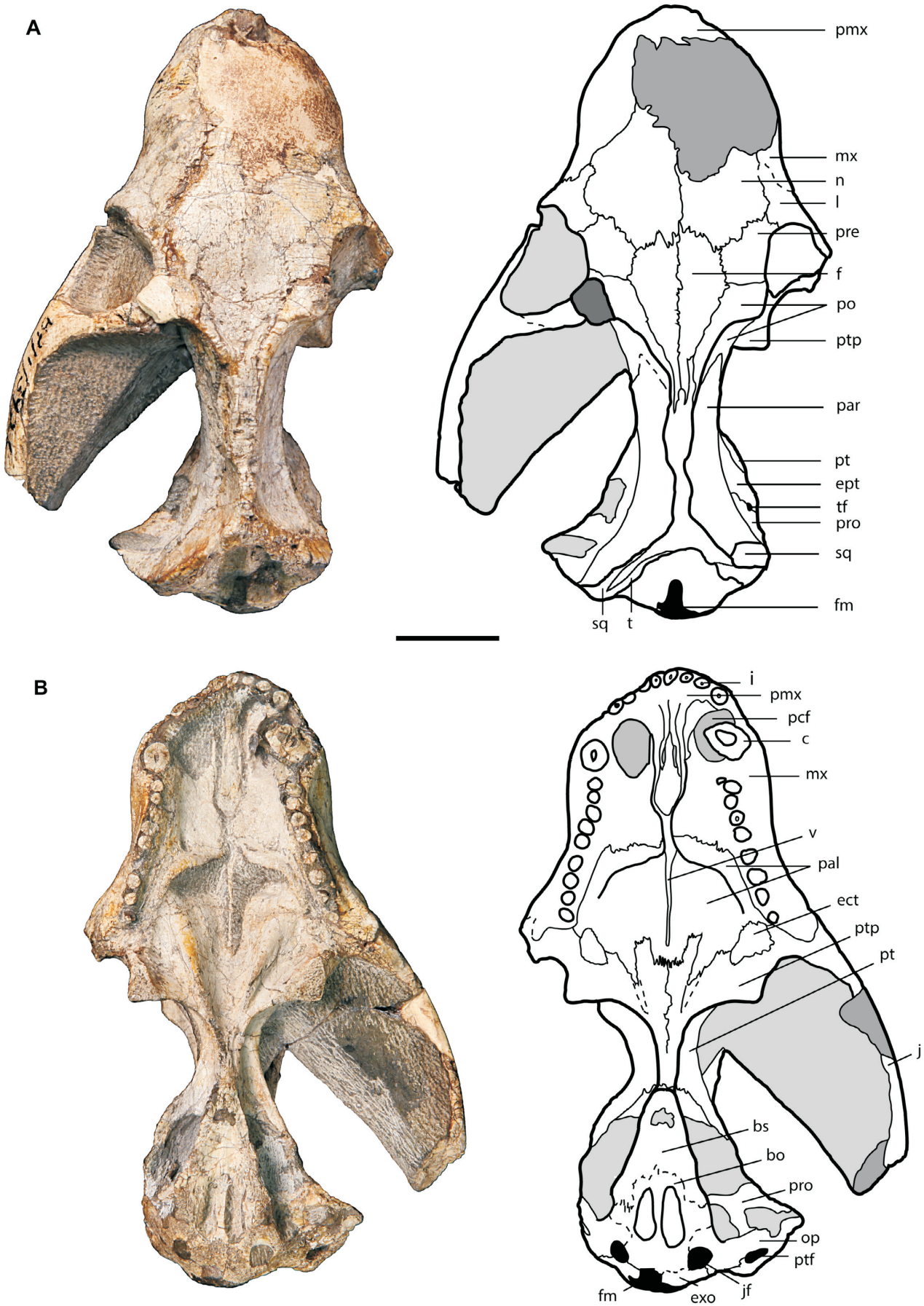


Figure 5. Photograph and interpretive drawing of *Cynosaurus suppostus*, specimen BP/1/3926, **A**, in ventral view, and **B**, in right lateral view. Abbreviations: **bo**, basioccipital; **bs**, basisphenoid; **c**, canine; **ect**, ectopterygoid**; ept**, epipterygoid; **exo**, exoccipital; **f**, frontal; **fm**, foramen magnum; **i**, incisor; **j**, jugal; **jf**, jugular foramen; **l**, lacrimal; **mx**, maxilla; **n**, nasal; **op**, opisthotic; **pal**, palatine; **par**, parietal; **pcf**, paracanine fossa; **pmx**, premaxilla; **po**, postorbital; **pre**, prefrontal; **pro**, prootic; **pt**, pterygoid; **ptf**, post-temporal fenestra; **ptp**, pterygoid process; **so**, supraoccipital; **sq**, squamosal; **tf**, trigeminal foramen; **v**, vomer. Scale bar equals 20 mm.

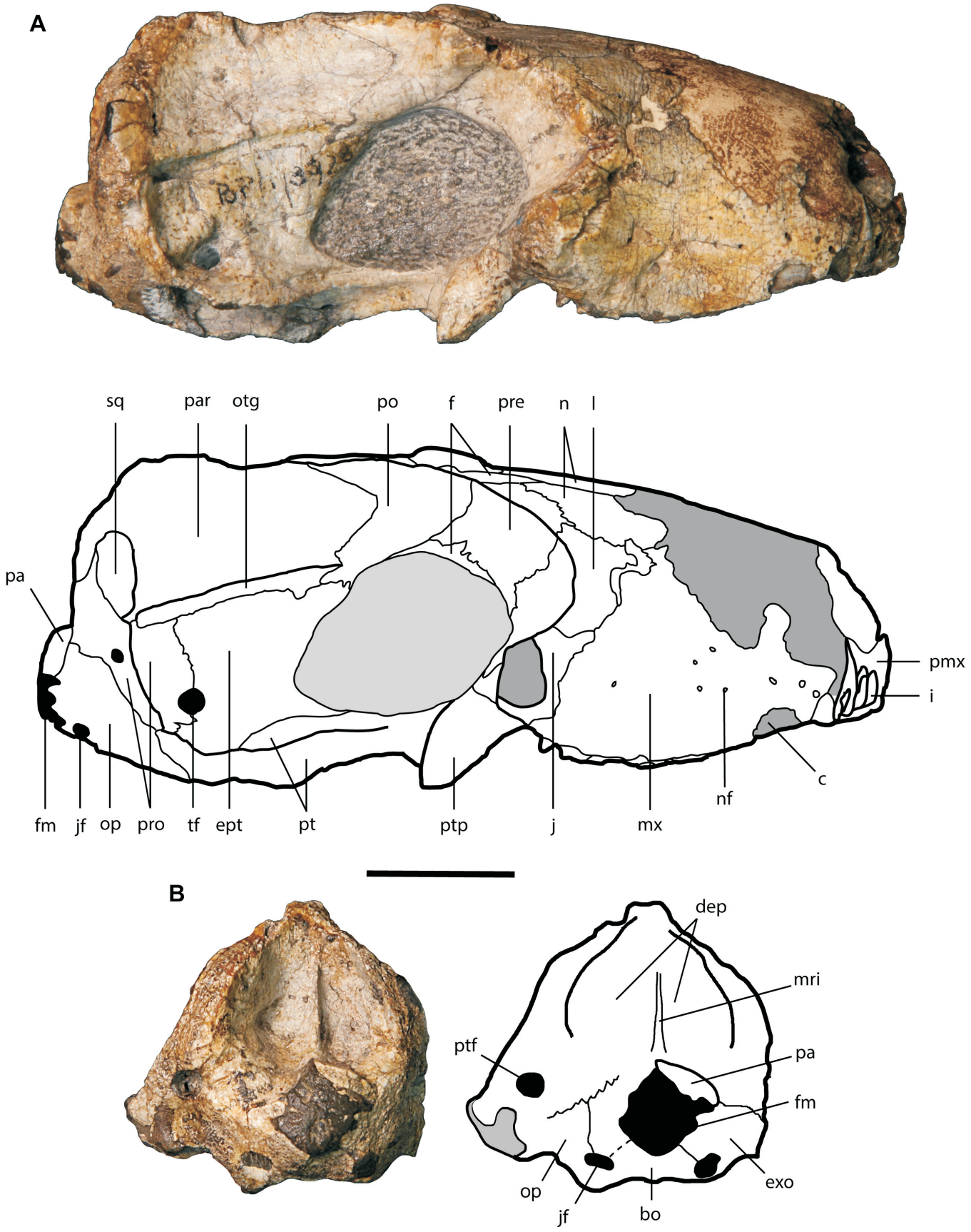


Figure 6. Photograph and interpretive drawing of *Cynosaurus suppostus*, specimen BP/1/3926, **A**, in right lateral view and **B**, in occipital view. Abbreviations: **c**, canine; **dep**, depression; **ept**, epipterygoid; **f**, frontal; **fm**, foramen magnum; **i**, incisor; **j**, jugal; **jf**, jugular foramen; **l**, lacrimal; **mri**, median ridge; **mx**, maxilla; **n**, nasal; **op**, opisthotic; **otg**, orbitotemporal groove; **pa**, proatlas; **par**, parietal; **pmx**, premaxilla; **po**, postorbital; **pre**, prefrontal; **pro**, prootic; **pt**, pterygoid; **ptf**, post-temporal fenestra; **ptp**, pterygoid process; **so**, supraoccipital; **sq**, squamosal; **t**, tabular; **tf**, trigeminal foramen; **v**, vomer. Scale bar equals 20 mm.

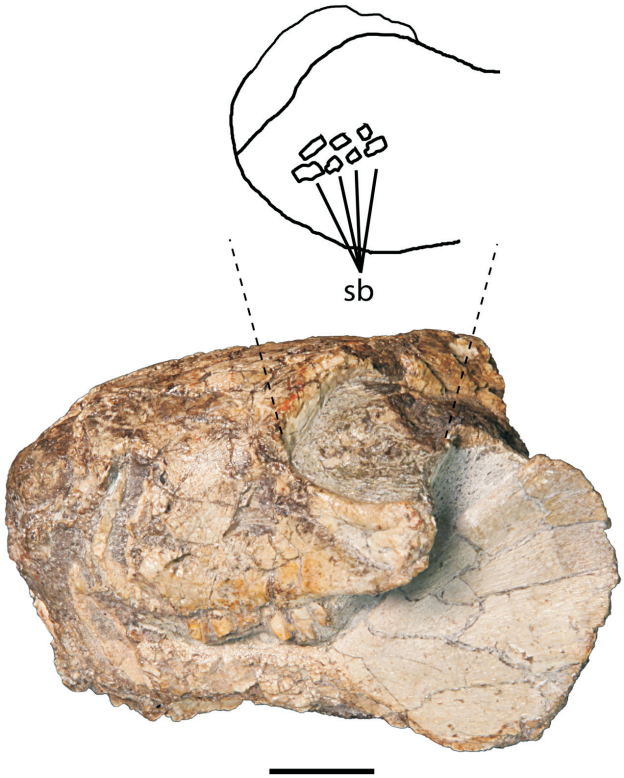


Figure 7. Scleral ossicles in the left orbit of *Cynosaurus suppostus*, specimen AM4947, photograph and interpretive drawing. Abbreviations: **sb**, scleral ossicles. Scale bar equals 1 cm.

fenestra is wide, being of equal width throughout its anteroposterior length.

Squamosal

The squamosal is a large bone forming the posterodorsal portion of the zygomatic arch anteriorly, the posterolateral portion of the occipital crest posteriorly and the squamosal portion of the posterolateral occipital region. This bone contacts the jugal anteriorly and anteroventrally, the parietal posteromedially, and the tabular posteriorly.

In BP/1/4469, the squamosal makes up the smaller portion of the zygomatic arch and extends posterolaterally outwards in a convex shape. The dorsal margin of the squamosal portion of the zygomatic arch continues dorso-medially to form the dorsal margin of the occipital crest. The squamosal overlaps the parietal on the proximal surface of the occipital crest.

Parietal

The parietal is a large bone and is located on the medial surface of the temporal fenestra. The parietal contacts the frontal anteriorly, the postorbital anterolaterally, the occipital crest of the squamosal posterolaterally and postparietal posteriorly.

In dorsal view, the bilaterally symmetrical parietals fuse on their midline to form a thin sagittal crest, present in both small and large specimens (Figs 5A, 9A). This crest is anteriorly wide and tapers posteriorly towards the pineal foramen (only represented in juvenile skulls), then maintaining a consistent narrow width beyond the pineal foramen until reaching the posterior margin of the parietal. The sagittal crest is elongate and narrow with deep lateral vertical faces, and does not rise in relation to the dorsal margin of the skull (Fig. 6A). The intertemporal region is narrower in the larger specimen BP/1/3926 (Figs 2E, 5), than in the smaller specimens (Figs 2A–B, 9A).

The pineal foramen is small and clearly present in the small specimen BP/1/1563 (Fig. 9A), and also appears to be present in the small specimen BP/1/4469 (Fig. 2B). However, identification in the latter is uncertain due to damage in the area where the foramen is located. In the large specimen BP/1/3926, damage to the sagittal crest precludes clear identification of a pineal foramen, but Brink (1965: 121) maintained that the slight swelling in the posterior parietal crest indicates the approximate location of the foramen. Benoit *et al.* (2015) conducted computed tomography (CT) scanning of this specimen and found no evidence of an internal parietal tube below the dorsal external swelling, indicating the absence of a pineal foramen in adult *Cynosaurus*. We agree with Benoit *et al.* (2015) that adult specimens of *Cynosaurus* lack a pineal foramen.

Posterior to the level of the pineal foramen, the sagittal crest divides into two lateral crests or flanges, the occipital crests (Figs 5A, 9A). These thin crests are vertically oriented and formed by two layers of bone, the anterior portion composed of the squamosal and the posterior portion of the postparietal mediodorsally and the tabular laterally.

Palate

Premaxilla

A large paracanine fossa is located anteromedially to each upper canine. The anterior margin of the paracanine fossa is formed by the premaxilla, and the posterior by the maxilla (Fig. 5B). There is a gap along the midline between the premaxillary palatal processes (Figs 5B, 9B).

Vomer

The vomer is unpaired and forms a medially-located vertical septum that extends anteroposteriorly. This bone contacts the premaxilla anteriorly and the palatines posteriorly. The vomer is observed in the gap between the palatal processes of the premaxillae (Figs 5B, 9B) and continues posteriorly in the gap formed between the palatal processes of the maxillae and palatines, emerging posteriorly beyond the palatal processes of the palatines. Posterior to the palatal processes, the vomer tapers until reaching a sharp point on the palatine, at a point roughly in line with the last postcanine. The vomer does not reach the pterygoid posteriorly (Fig. 5B).

In the small specimen BP/1/1563, the vertical septum of the vomer is exposed between the palatal processes of the maxilla and the palatine and shows a well-developed, distinct, deep channel on its ventral surface.

Maxilla

The maxilla forms the anterior portion of the incomplete secondary palate, contacting the premaxilla anteriorly and the palatine posteriorly. The palatal processes of each maxilla do not meet in the midline (Figs 5B, 9B). The incisive foramina are not closed by the palatal processes of

the maxilla. The narrowest point of the incisive foramen is posterior to the level of the paracanine fossa. In smaller specimens, the gap between the edges of the incomplete secondary palate is proportionally wider than in larger specimens (Figs 5B, 9B). A large posterior palatal foramen is located anterolaterally to the maxillary-palatine suture (Fig. 9B).

Palatine

The palatine forms a large portion of the palate. This bone contacts the maxilla anteriorly and the pterygoid posteriorly. The anterior contact between the maxilla and palatine occurs on the secondary palate, whereas the posterior contact between the palatine and the pterygoids occurs immediately posterior to the posterior edge of the vomer. Posterolateral to the vomer, a posteromedially-oriented palato-pterygoid crest rises from the palatine, tapering dorsally to a thin sharp edge. The dorsal, thin, sharp edge of this crest is contributed by the palatine, whereas the more ventral underlying body of the crest is formed by the pterygoid. The sutures between the palatine and pterygoid occur along the rising medial surface of the crest (Fig. 5B).

The palatal plates of the palatine do not meet in the midline but contribute to the posterior portion of the incomplete secondary palate (Figs 5B, 9B). The palatal processes of the palatine are short in relation to the overall secondary palate length, as the maxilla contributes the greatest length. The posterior edge of the bony secondary palate on the palatine forms a curved, arch-shaped margin and extends laterally to reach a point just anterior to the last upper postcanine (Fig. 5B).

Ectopterygoid

The small ectopterygoid is located anterolaterally to the pterygoid process, contacting the flange posteriorly (Fig. 5B). The ectopterygoid contacts the palatine anteriorly. A single large foramen is identifiable on the right ectopterygoid in AM4947, where the ectopterygoid-pterygoid suture is clear.

Pterygoid

The pterygoid is a large bone forming the posterior portion of the primary palate region, contacting the palatines anteriorly and extending posteriorly towards the basicranium to contact the basisphenoid posteriorly and the quadrate via the quadrate ramus of the pterygoid, posterolaterally (Fig. 5B).

Anteriorly, the pterygoids form the transverse flange or pterygoid process, located posterolaterally to the palatine crests (Fig. 5B). In ventral view, the pterygoid processes thin laterally and taper medially. The posterior margins of the pterygoid processes are vertically oriented.

The interpterygoid vacuity is present in the small specimen BP/1/1563 (Fig. 9A), but is not present in the larger specimens. This ontogenetic loss of the paired interpterygoid vacuities has also been reported in *Thrinaxodon* (Jasinoski *et al.* 2015), whereas vacuities are absent altogether in *Galesaurus* (Jasinoski & Abdala 2017).

The posterior part of the pterygoid and the rostrum of the parasphenoid form the basicranial girder. This portion of the pterygoid tapers initially medially to reach its narrowest width, after which it expands laterally to contact the basisphenoid (Fig. 5B).

Basicranium

The basicranium is a triangular structure relatively longer than wide (Figs 5B, 9B).

Basisphenoid

The basisphenoid forms the anterior portion of the basicranium and is roughly triangular with the apex pointing anteriorly. The surface of this bone is generally flat, but it has a shallow fossa covering the majority of the central portion of the bone. This depression has a faint median ridge running through the centre, which is most visible in the small specimen BP/1/1563 (Fig. 9B). In this specimen, the outer circular edges of the fossa are slightly raised above the level of the surrounding bone.

Basioccipital

The basioccipital is roughly circular in shape, having an anterior contact with the basisphenoid in the form of an inverted U-shape medially. The basioccipital tapers anteriorly and broadens posteriorly. A deep parasagittal depression covers the majority of the bone (Fig. 5B). This depression has a strong central ridge running through the centre of the bone. The outer circular edges of the parasagittal depression are slightly raised above the level of the surrounding bone. This parasagittal depression is much deeper in the larger specimen BP/1/3926 (Fig. 5B).

Quadrate and quadratojugal

The quadrate and quadratojugal are only observable in the small specimen BP/1/4469 and are best observed on the occiput (Fig. 8B), although the quadrate is still mostly obscured by matrix. The quadratojugal is represented by the ascending process: a thin splint of bone, oriented vertically, located on the lateroventral edge of the occiput. Medial to this bone, the squamosal forms the quadrate notch medially and the quadratojugal notch laterally. The quadratojugal contacts the articular ventrally at the same height as the postcanine tooth row.

Prootic

The prootic forms the anterior part of the wall of the fenestra ovalis, whereas the opisthotic forms the posterior margin of this opening. The lateral flange of the prootic is present in BP/1/3926 (Fig. 5B).

In BP/1/1563, the basisphenoid wing or parasphenoid ala is long, extending posteriorly, but does not contribute to form the margin of the fenesta ovalis. The cavum epiptericum is open ventrally (Fig. 9B). The fenestra ovalis is located anterolaterally to the jugular foramen (Fig. 9B). Anterior to the fenestra ovalis, a small primary facial foramen is observed on the prootic, along with a small, anteroposteriorly-oriented crest separating the fenestra ovalis from the cavum epiptericum. The primary facial foramen is proportionally much larger in the small specimen BP/1/1563.

Opisthotic

The opisthotic forms the anterolateral rim and the exoccipital forms the posterior rim of the jugular foramen in BP/1/3926 (Fig. 5B). In ventral view on BP/1/4469, the paroccipital process appears as a rectangular projection. This process is latero-medially elongated and widens laterally. The paroccipital process appears to contact the quadrate on the left side in BP/1/4469.

Lateral wall of the braincase

Prootic

In lateral view, the prootic is located on the posterior part of the lateral wall of the braincase, ventral to the parietal, and contributes to the posterior margin of the very large trigeminal foramen, with the epipterygoid forming the anterior margin (Figs 6A, 9C).

Epipterygoid

The epipterygoid is an anteroposteriorly elongate, thin bone, situated dorsal to the quadrate ramus of the pterygoid. The epipterygoid bears a long anterior extension or ascending process dorsally.

In BP/1/3926, the orbito-temporal groove forms a well-defined, long, horizontal channel between the parietal dorsally and the prootic and epipterygoid ventrally. This forms a shallow furrow on the parietal, and extends from its anterior contact with the postorbital to the level of the trigeminal foramen posteriorly (Fig. 6).

Occiput

The occiput of the large specimens is relatively wide, broad, flat, and oriented vertically, whereas in the small specimens the occiput slopes anteriorly. The sutures of the occipital plate are difficult to identify in the large specimen BP/1/3926 (Fig. 6B) and are best exposed in the small specimen BP/1/4469 (Fig. 8B).

Postparietal

The postparietal is a vertically-oriented bone located on the dorsal medial portion of the occiput, which contacts the tabulars laterally and the supraoccipital ventrally. Dorsally, the postparietal forms a small pentagonally-shaped wedge of bone, reaching the parietal on the sagittal crest, just posterior to the pineal foramen in the small specimens (Fig. 8B). The postparietal features a shallow parasagittal depression, separated by a faint vertically-oriented median ridge. In BP/1/3926, this depression is much deeper and the median ridge is much more sharply raised and pronounced (Fig. 6B).

Supraoccipital

The supraoccipital is a relatively wide bone, forming the dorsal margin of the foramen magnum (Figs 8B, 9E), and broadens ventrally, reaching its widest point ventrolaterally at the ventralmost contacts with the tabulars.

The vertically-oriented median ridge running through the centre of the postparietal extends ventrally onto the surface of the supraocciptal (Fig. 6B). As is the case on the postparietal, the ridge size and extension onto the supraocciptal is more pronounced in the large specimen BP/1/3926.

Tabulars

The tabulars are located on the dorsolateral portion of the occiput, contributing to the occipital crests. The tabular makes a small contact with the paroccipital process of the opisthotic ventrally, between the squamosal and the

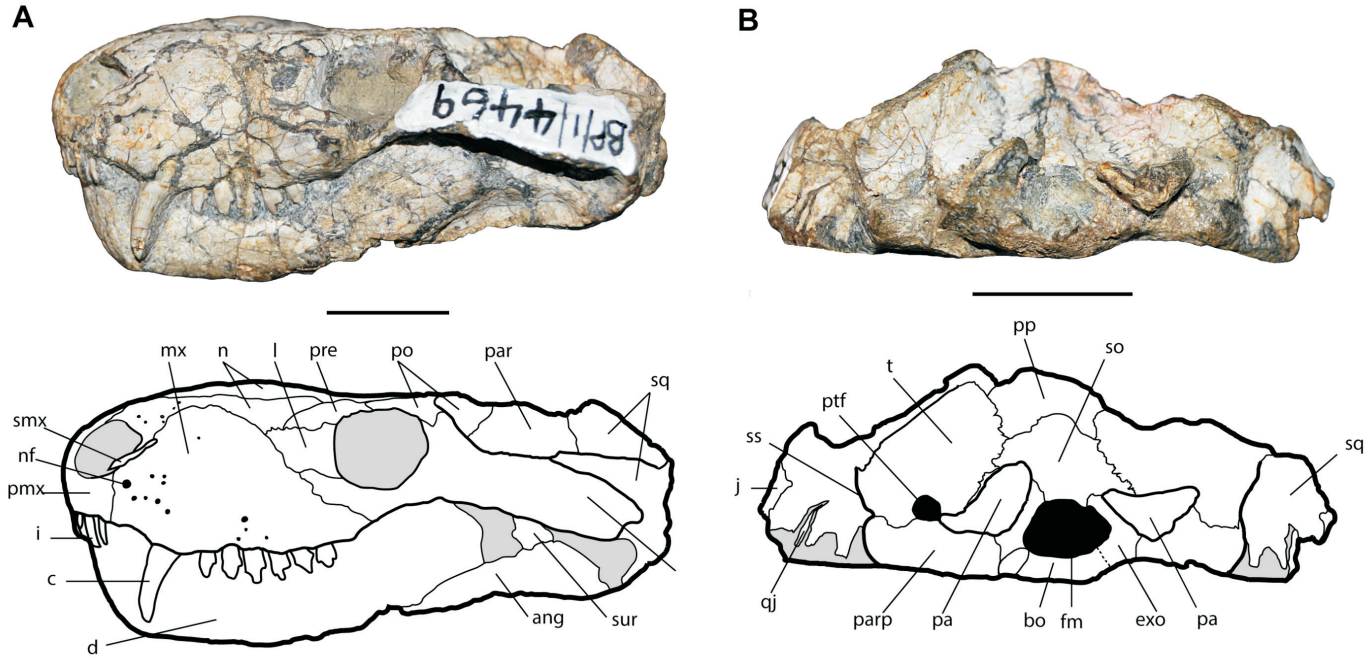


Figure 8. Photograph and interpretive drawing of *Cynosaurus suppostus*, specimen BP/1/4469, **A**, in left lateral view and **B**, in occipital view. Abbreviations: **ang**, angular; **bo**, basioccipital; **c**, canine; **d**, dentary; **fm**, foramen magnum; **i**, incisor; **j**, jugal; **l**, lacrimal; **mx**, maxilla; **n**, nasal; **nf**, nutritive foramina; **pa**, proatlas; **par**, parietal; **parp**, paroccipital process; **pmx**, premaxilla; **po**, postorbital; **pp**, postparietal; **pre**, prefrontal; **ptf**, post-temporal fenestra; **qj**, quadratojugal; **smx**, septomaxilla; **sq**, squamosal; **ss**, squamosal sulcus; **sur**, surangular; **t**, tabular. Scale bar equals 10 mm.

exoccipital (Fig. 8B). The tabular is in contact with the squamosal via the squamosal sulcus ridge (Fig. 8B). The tabulars form the lateral and dorsal borders of the post-temporal fenestra (Fig. 9E) and the paroccipital process appears to form the base. However, there is a thin horizontal piece of bone also at the base of the fenestra, which could be part of the tabular (Figs 6A, 8B). The post-temporal fenestra is much smaller than the foramen magnum (Figs 6B, 8B, 9E).

Squamosal

The squamosal is positioned laterally in the occiput and contacts the tabulars medially, at the junction of the zygoma and occipital crests (Figs 8B, 9E). In occipital view, a shallow V-shaped notch is formed by the dorsal surface of the medial tabular part of the occipital crest and the dorsal surface of the lateral squamosal part of the zygoma. The squamosal sulcus is a vertically-oriented ridge running along the squamosal-tabular contact that forms a moderately deep vertical groove, ending behind the quadrate (Fig. 8B). There is no posterior horizontal projection of the squamosal dorsal to the squamosal sulcus.

Basioccipital

The basioccipital forms the ventral rim of the foramen magnum, medial to the double occipital condyles of the exoccipitals (Fig. 8B). The exoccipital contacts the tabulars dorsally and ventrally forms the occipital condyles. The exoccipitals also make up the lateral margins of the foramen magnum.

Proatlas

A right partial proatlas is preserved in BP/1/3926 (Fig. 6B) and is located on the right dorsal margin of the foramen magnum. In specimen BP/1/4469, both proatlantes are preserved, the left being better preserved (Fig. 8B). In dorsal view, the proatlas is rectangular in shape, wider proximally, and the distal lateral margin is curved 90° compared to the rest of the bone.

Lower jaw

The mandible is robust in *Cynosaurus*, with the horizontal ramus very high and the mentum subvertical.

Dentary

The left and right dentaries are unfused at the symphysis in both large (e.g. SAM-PK-K10694) and small (e.g. BP/1/4469) specimens. In lateral view, the symphysis is anteriorly convex in specimen BP/1/4469 (Fig. 8A). The lateral surface of the horizontal ramus of the dentary is generally smooth and almost flat, but the anterior portion posterior to the level of the canines is slightly concave. The ramus maintains a relatively equal height over most of its extension and bends sharply upwards posterior to the last postcanine, at the level of the anterior margin of the orbits, producing the coronoid process. The anterior margin of this process is mediolaterally thickened. The coronoid process slopes posterodorsally and presents a shallow depression, the masseteric or adductor fossa, on its lateral surface. In BP/1/4469, the fossa is present as a wide depression separated by a posterodorsally-oriented lateral crest or sharp ridge that runs through the middle of the coronoid process. This well-developed ridge extends onto the angle of the dentary, dividing the fossa into distinct dorsal and ventral portions. The ventral portion extends ventrally onto the angle of the dentary. The situation is similar in the mandible of AM4947, but the lateral crest is broad and slightly raised (Fig. 7).

The articular process of the dentary is poorly developed. In BP/1/4469 (Fig. 8A), the angular process of the dentary is

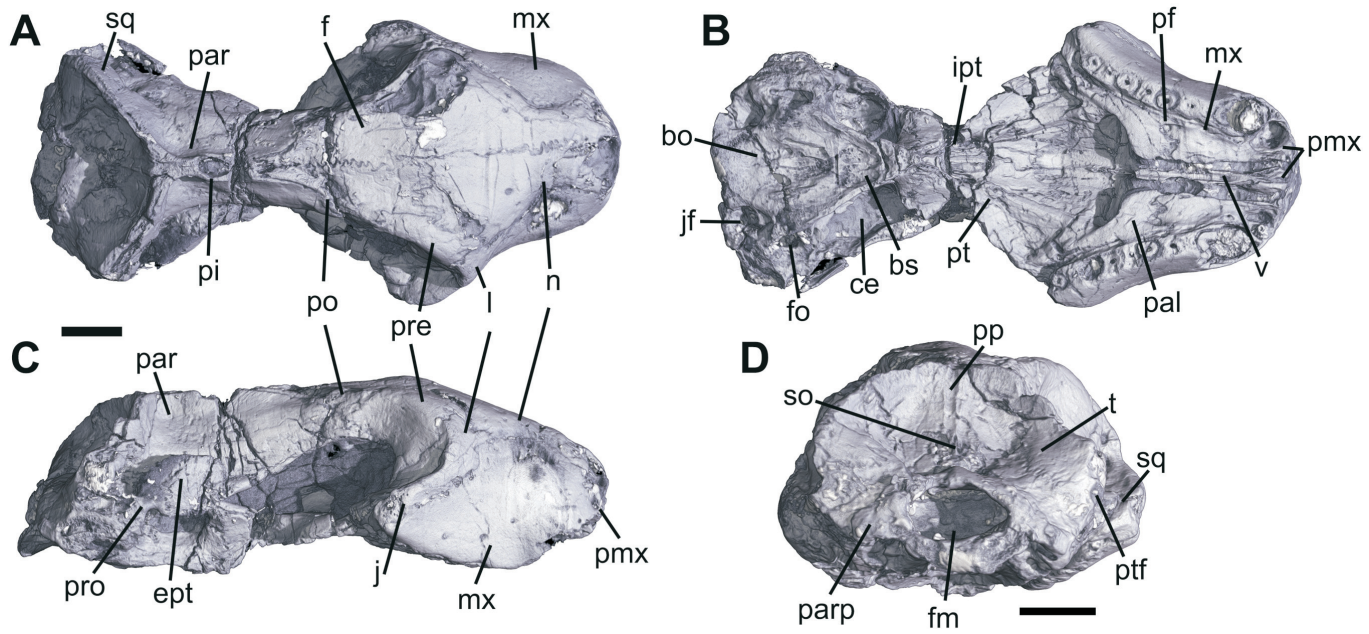


Figure 9. Virtual reconstruction of *Cynosaurus suppostus*, specimen BP/1/1563, **A**, in dorsal view, **B**, in ventral view, **C**, in right lateral view, and **D**, in occipital view. Abbreviations: **bo**, basioccipital; **bs**, basisphenoid; **ce**, cavum epiptericum; **ept**, epipterygoid; **f**, frontal; **fo**, fenestra ovalis; **fm**, foramen magnum; **j**, jugal; **jf**, jugular foramen; **ipt**, interpterygoid vacuity; **l**, lacrimal; **mx**, maxilla; **n**, nasal; **pal**, palatine; **par**, parietal; **parp**, paroccipital process; **pf**, palatal foramen; **pi**, pineal foramen; **pmx**, premaxilla; **po**, postorbital; **pp**, postparietal; **pre**, prefrontal; **pro**, prootic; **pt**, pterygoid; **ptf**, post-temporal fenestra; **so**, supraoccipital; **sq**, squamosal; **t**, tabular; **v**, vomer. Scale bar equals 5 mm.

not completely preserved on the left and is better preserved and more complete on the right side. On both sides it forms a relatively distinct and sharply angled keel/heel upwards at approximately 30° from the horizontal (Fig. 8A). The angular process of the dentary is located at the level of the postorbital bar.

Angular

The angular is only preserved in BP/1/4469 (Fig. 8A). This bone forms the ventral posterolateral portion of the mandible and is located ventrally to the coronoid process of the dentary, forming a concave lamina. The angular contacts the base of the coronoid process of the dentary dorsally and the articular posteriorly. The reflected lamina of the angular is not preserved in any specimen. Part of the surangular is exposed posteriorly in BP/1/4469, but it is not possible to see the suture between the surangular and angular.

Articular-prearticular

In ventral view, the articular-prearticular bar is an anteroposteriorly raised bar, running along the medial margin of the angular. Posteriorly, the bone widens to stretch between the lateral and medial surfaces of the ventral mandible margin, forming a triangular shape. In ventral view, in BP/1/4469, the articulars are observed as smooth flattened areas of bone with slightly concave surfaces for articulation to the quadrate trochlea of the cranium.

Splenial

The splenial is a thin, elongated vertical lamina located medial to the dentary. In AM4947, the splenial continues posteriorly, well beyond the level of the pterygoid processes, as a shallow, thin bone limited to the medial surface of the mandible.

Dentition

Dental formula and preservation

The dental formula of *Cynosaurus* is I4/i3, C1/c1, PC6-9/pc6-9 and the adult formula is I4/i3, C1/c1, PC8-9/pc8-9 (Table 3). The upper tooth row extends posteriorly to just beyond the level of the anterior margin of the orbits. There is no evidence for occlusion, as the surfaces of the upper and lower teeth lack wear facets.

Incisors

Upper incisors number four on both sides in almost all specimens where they are preserved (Table 3). The number of incisors is peculiar in SAM-PK-K10694, a large specimen, which preserves five right and four left upper incisors (Fig. 10C). The additional right incisor may represent the retention of a replacement tooth. There are three lower incisors in the small specimen BP/1/4469, as revealed by CT-scanning. However, based on alveolar count, there are only two lower incisors on either side in the large specimen SAM-PK-K10694.

The upper incisors are pointed and conical, without serrations. In the larger specimens, all incisors are of similar width and length, with no marked differences between them. The small specimen BP/1/4469 shows variation in size and length, with the left second tooth being very small, possibly due to it being newly erupted (Fig. 10F). In SAM-PK-4333 (Fig. 1D), each incisor shows several deep, ridged, longitudinal grooves or striations. These longitudinal grooves also occur over the entire length of the crown in SAM-PK-K10694 (Fig. 10C) and BP/1/4469 (Fig. 10F).

The incisors are vertically oriented and point slightly backwards in the small specimen BP/1/4469 (Fig. 10F).

In BP/1/3926 (Fig. 5B), the incisor crowns are not preserved, but the cross-section reveals variation from spherical to oval and the damaged left upper incisors in SAM-PK-K10694 are oval in cross-section.

A diastema of approximately 4mm between the last incisor and the canine is observed on both sides of the larger specimens SAM-PK-4333 (Fig. 1D) and BP/1/3926 (Fig. 5B). In SAM-PK-K10694, the diastema is also approximately 4–5 mm, but a portion of the diastema is occupied by small canine replacement teeth, located immediately anteriorly to each upper canine (Figs 4A, 10C).

Canines

There are single upper and lower canines, oval in cross-section, which are anteroposteriorly elongated and unserrated. They have a convex anterior and a concave posterior edge, and have several longitudinal grooves or striations occurring over the entire length of the crown, most clearly seen in SAM-PK-K10694 (Fig. 10A–C) and BP/1/4469 (Fig. 10D–F). The upper canines show a distinct posterior ridge in SAM-PK-K10694.

In SAM-PK-K10694, small canine replacement teeth are located immediately anteriorly to each upper canine (Fig. 10A–C), whereas in the small specimen BP/1/1563, canine replacement teeth are located immediately posterior to each canine.

Postcanines

Upper and lower postcanines number seven to eight in most specimens (Table 3). However, there are only six upper postcanines in the small specimen BP/1/4469 (Fig. 10D, E) and the first, fifth, and sixth postcanines are smaller than the second, third and fourth. The large specimen BP/1/3926 has nine upper postcanines (Fig. 5B), with

Table 3. Dentition count, right and left respectively, of SAM-PK-4333, SAM-PK-K10694, BP/1/3926, AM 4947, BP/1/4469 and BP/1/1563.

Element	Dentition	SAM-PK-4333	SAM-PK-K10694	BP/1/3926	AM 4947	BP/1/4469	BP/1/1563
Maxilla	Insisors	4, 4	5, 4	4, 4		4, 4	
Maxilla	Postcanines	8, 8	8, 8	9, 9	8, 7	6, 6	7, 7
Mandible	Insisors		2?, 2?			3, 3	
Mandible	Postcanines		6, 8			7, 7	

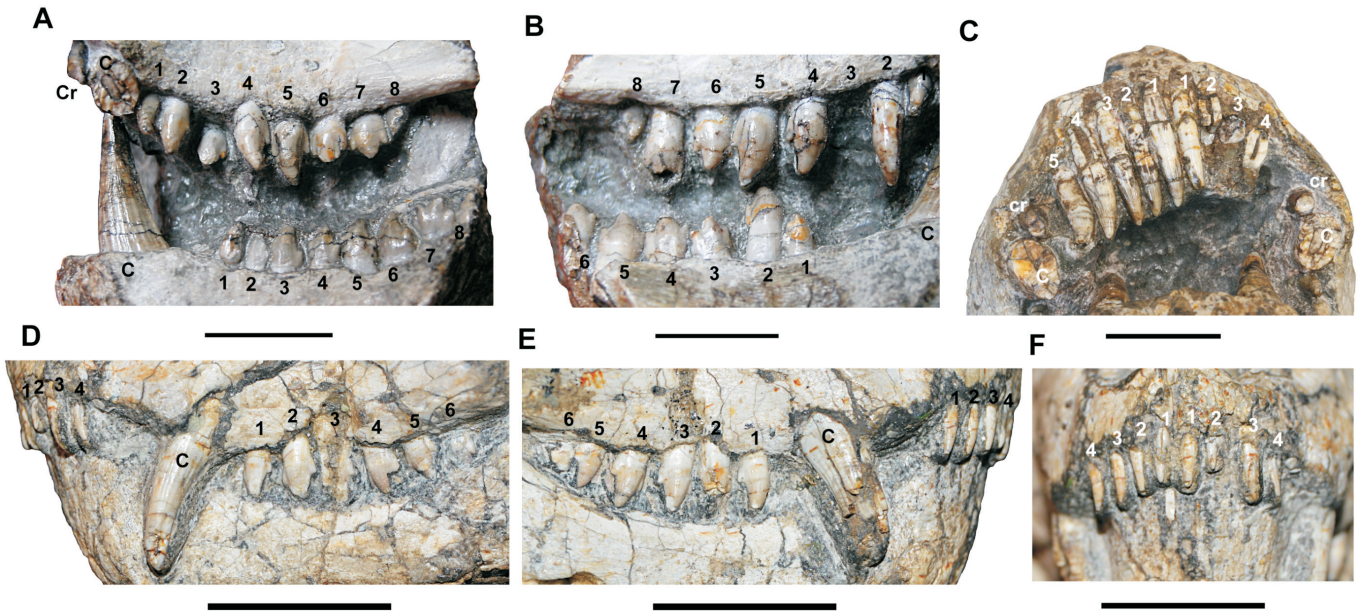


Figure 10. Upper and lower dentition of *Cynosaurus suppostus*, specimens SAM-PK-K10694 and BP/1/4469. **A**, SAM-PK-K10694 in left lateral view, **B**, in right lateral and **C**, in anterior views. Specimen BP/1/4469 in **D**, left lateral and **E**, right lateral views. Arabic numbers indicate postcanines in (A), (B), (D) and (E) and incisors in (C). Abbreviations: **C**, canine; **cr**, canine replacement. Scale bar equals 10 mm.

the same pattern of tooth sizes as the first and last two postcanines as the smallest.

The postcanine morphology consists of a slightly curved main cusp per tooth, with a variety of anterior and posterior accessory cusps which differ in their number and placement. The external surfaces are smooth, with no cingula or cingular cusps present. In general, the postcanine teeth exhibit one of two morphological conditions: 1) the first and second postcanines have a main recurved cusp with a convex anterior edge and with a single posterior accessory cusp, or 2) from the third postcanine backwards, the postcanines have a main recurved cusp, with a single anterior and a single posterior accessory cusp.

The large specimen SAM-PK-K10694 provides the best preserved and most complete postcanine dentition of all specimens. In this specimen (Fig. 10A–C), the first upper postcanine (PC) is small, simple and pointed and bent slightly backwards. The PC2 has a straight main cusp, with a slight posterior ledge, but no true cusp (on the right side), or a small posterior accessory cusp (on the left side). The PC3 on the left side is an erupting postcanine tooth deeply set in the maxilla, with a recurved main cusp and a small posterior accessory cusp. The PCs 4 and 5 show recurved main cusps with small single posterior accessory cusps, whereas PCs 6 and 7 show recurved main cusps with equally-sized small single anterior and posterior accessory cusps. The PC8 is broken off on the left, and the right side is very small and shows a recurved main cusp with a small posterior accessory cusp. The first lower postcanines (pc) of SAM-PK-K10694 are separated from the canines by a diastema of 4mm (Fig. 10A–B). On the left side, pcs 1 to 3 show a recurved main cusp with single posterior accessory cusp each. The pcs 4 to 6 show a recurved main cusp with single anterior and posterior accessory cusps, the anterior being more developed than the posterior. The pc7 shows a recurved main cusp, a single posterior accessory cusp and two anterior accessory cusps. On the right side, the pcs 1 and 2 consists of a single recurved main cusp, with a single posterior accessory cusp. The pcs 3 to 6 show single recurved main cusps, with single anterior and posterior accessory cusps, the anterior being more developed than the posterior.

In AM4947, the upper left postcanines are damaged, but PCs 4 to 6 show a recurved main cusp with single posterior accessory cusps. In addition, the fourth postcanine also exhibits a single anterior accessory cusp. The upper right postcanines consist of a recurved main cusp only, with PCs 5 to 8 also showing single posterior accessory cusps. In the small specimen BP/1/4469 (Fig. 10D, E), the first PC on both sides displays a single recurved main cusp with a small posterior accessory cusp. The PCs 2 to 6 have recurved main cusps, with single anterior and posterior accessory cusps, with the anterior accessory cusps being better developed than the posterior ones.

DISCUSSION

Comparisons with other basal cynodonts

When compared with other basal (non-eucynodont) cynodonts, the most important diagnostic characters in *Cynosaurus* are represented in the snout. *Cynosaurus's* snout length (obtained from the average of the two large specimens BP/1/3926 and SAM-PK-4333) is approximately 38% of the basal skull length (Table 4). This is the second shortest snout among basal cynodonts, very close to *Progalesaurus* at 37% and also to the 39% of *Platycraniellus*. Other basal cynodonts have proportionally longer snouts: *Procynosuchus* at 45%, *Galesaurus* at 43% and *Thrinaxodon* at 44% (Table 4). As well as being short, *Cynosaurus* has the proportionally broadest snout, at approximately 32% of basal skull length, for the large complete and undistorted specimen BP/1/3926 (with the closest other taxon being *Platycraniellus* at 30%) (Table 4). The *Cynosaurus* specimen

Table 4. Measurements (in cm) of the basal skull length (BSL), snout width (SW), snout length (SL) and the percentages of the ratio between snout width and the basal skull length (SW/BSL) and snout length and basal skull length (SL/BSL). Measurements by Fernando Abdala.

Taxon	Specimen	BSL	SW	SW/ BSL	SL	SL/ BSL
Cynosaurus	BP/I/3926	11.52	3.65	32%	4.44	39%
	SAM-PK-4333	12.16			4.59	38%
	Average					**38%**
Platycraniellus	TM 25	8.4	2.5	30%	3.3	39%
Progalesaurus	SAM-PK-K9954	9.35	2.47	26%	3.45	37%
Galesaurus	SAM-PK-K9456	7.3	1.9	26%	3.29	45%
	AMNH 2227	7.9	1.7	22%	3.71	47%
	NMQR 1451	9	2.4	27%	3.51	39%
	SAM-PK-K-9454	9.2	2.5	27%	3.77	41%
	AMNH 2223	10	2.9	29%	4.10	41%
	NMQR 3340	10.1	2.3	23%	4.55	45%
	BP/1/5064	10.3	3	29%		
	NMQR 860	11.4	3.2	28%	4.79	42%
	Average			**26%**		**43%**
Procynosuchus	BP/1/591	8.3	2.3	28%	3.7	45%
	BP/1/2600	8.6	2.7	31%	4.3	50%
	BP/1/226	8.7	2.3	26%	3.8	44%
	RC 72	8.8	1.9	22%	3.9	44%
	RC 87	10.5	2.6	25%	4.4	42%
	RC 12	10.6	2.7	25%	5	47%
	OUM.TSK 34	11.1	2.4	22%	5.6	50%
	RC 130	12.3	2.8	23%	5.9	48%
	RC 5	12.9	3.3	26%	5	39%
	BP/1/3748	14.2	3.8	27%	6.6	46%
	RC 92	14.4	3.9	27%	6.4	44%
	Average			**26%**		**45%**
Thrinaxodon	BP/1/5372	3.6	1	28%	1.6	44%
	BSP 1934 VIII 506	6.1	1.6	26%	2.5	41%
	BP/1/4280	6.1	1.7	28%	2.8	46%
	NMQR 812	6.4	1.7	27%		
	NMQR 24	6.4	1.5	23%	2.9	45%
	NHMUK R3731	7.1	2	28%	3	42%
	SAM PK-K-1498	7.2	1.9	26%	3.2	44%
	SAM PK-K1499	7.5	2.1	28%		
	BP/1/5208	7.6	2	26%	3.7	49%
	NHMUK R5480	7.8	2.2	28%	3.6	46%
	BP/1/4714	8.1	1.9	23%	3	37%
	BP/1/1375	8.1	2	25%	4	49%
	NHMUK R511	8.4	2	24%	3.7	44%
	BPI/1/2513a	8.9	2.5	28%	4.1	46%
	SAM PK-K-379	8.9	1.9	21%	3.9	44%
	SAM PK-K-1467	9.6	2	21%	3.9	41%
	NMQR 810	9.6	2.3	24%		
	UCMP 42866	7	1.7	24%		
	UCMP 42865	6.1	1.5	25%		
	UCMP 42877	4	1	25%		
	UCMP 42878	3.8	1	26%		
	AMMM 4283	8.5	2.2	26%		
	Average			**25%**	**44%**	

SAM-PK-4333 is crushed and distorted, so the estimated ratio of snout width to basal skull length in this individual (24.07%) is not reliable (Table 2). All other taxa compared have narrower snouts: *Procynosuchus*, *Progalesaurus* and *Galesaurus* at 26% and *Thrinaxodon* at 25% (Table 4).

In the orbital region of *Cynosaurus*, *Progalesaurus* and a few specimens of *Galesaurus*, the frontal forms a flat or slightly depressed region, below the level of the surrounding postorbital (Jasinoski & Abdala 2017), whereas in *Procynosuchus* and *Thrinaxodon* the frontal bears a medially raised ridge, which originates in the posterior part of the nasals and continues through to the frontals. In *Cynosaurus* and *Progalesaurus*, the posterior projection of the postorbital on the parietal forms a sharply forked shape with well-differentiated dorsal and ventral processes (Fig. 6). In the small specimen of *Cynosaurus* BP/1/4469 the ventral process is well preserved and longer than the dorsal process, although the dorsal process is somewhat eroded. In the large specimen BP/1/3926 these processes are more equal. Juveniles of *Thrinaxodon* and *Galesaurus* present a long ventral process and a short incipient dorsal process, whereas subadults and adults exhibit dorsal and ventral processes that produce a C-shaped bifurcated posterior projection (Jasinoski *et al.* 2015; Jasinoski & Abdala 2017).

In *Cynosaurus* and *Galesaurus*, the pineal foramen is large in juveniles. *Cynosaurus* closes the pineal foramen in adulthood (Benoit *et al.* 2015), an atypical condition amongst basal cynodonts, otherwise occurring only in eucynodonts (e.g. *Massetognathus*). *Galesaurus* specimens retain a very small pineal foramen into adulthood (Jasinoski & Abdala 2017) whereas the foramen remains large in adult *Thrinaxodon*, *Procynosuchus* and *Progalesaurus*. In *Cynosaurus*, *Platycraniellus*, *Procynosuchus* and *Thrinaxodon*, the sagittal crest is also developed in front of the pineal foramen. In *Thrinaxodon*, this anterior portion of the crest develops late in ontogeny and is only present in adult specimens (Jasinoski *et al.* 2015). In *Galesaurus* and *Progalesaurus* there is no sagittal crest formed in front of the pineal foramen, with the exception of one large *Galesaurus* skull (Jasinoski & Abdala 2017).

Interestingly, the *Cynosaurus* specimen AM4947 shows the presence of orbital scleral ossicles. These elements are more commonly recorded in basal therapsids (e.g. biarmosuchians, gorgonopsians and therocephalians). This is only the third record of scleral elements in non-mammaliaform cynodonts, the others being in a juvenile late Permian *Procynosuchus* and in a specimen of the Early Jurassic *Tritylodon* (Angielczyk & Schmitz 2014). The long phylogenetic and temporal ranges represented between species preserving scleral ossicles suggests that these elements are quite likely present in other non-mammaliaform cynodonts but not recovered in the fossil record. Unfortunately, only a few scleral ossicles are preserved out of place in the centre of the orbit in AM4947 (Fig. 7), so it is not possible to determine the type of visual activity in *Cynosaurus*.

The paired secondary palatal processes of the maxillae and palatine bones show a relatively narrow separation from one another in the midline posteriorly, which is

similar in *Cynosaurus* and *Galesaurus*. In *Procynosuchus*, the secondary palate is also incomplete, but the gap between the palatal processes of the maxillae and palatine bones is wider than the condition found in *Cynosaurus* or *Galesaurus*. In *Thrinaxodon* and *Platycraniellus*, the secondary palate is almost completely closed. Jasinoski *et al.* (2015) report the palatal shelves of *Thrinaxondon* as not tightly articulated along the midline and therefore not truly closed. The anteroventral margin of the vomer is broader than the open secondary palate cleft in *Cynosaurus* and *Galesaurus*.

The mandible of *Cynosaurus* is very robust and relatively high in relation to the length of the horizontal ramus, with a high, subvertical mentum. *Galesaurus* has a more gracile mandible, whereas those of *Procynosuchus* and *Thrinaxodon* are much more gracile and slender. In all of these taxa the mentum is shallower than in *Cynosaurus*.

In *Cynosaurus*, the masseteric fossa on the lateral surface of the dentary is made of dorsal and ventral portions separated by a coronoid eminence. In *Progalesaurus* and *Galesaurus*, this fossa is not well defined, but is also composed of dorsal and ventral portions, separated by a well-developed coronoid eminence. In *Procynosuchus*, *Dvinia* and *Abdalodon* the masseteric fossa is positioned on the dorsal portion of the coronoid eminence.

In the dentition, the canines of *Cynosaurus* and *Progalesaurus* present strong longitudinal grooves or striations that are also present but fainter in *Platycraniellus*, *Procynosuchus* and *Galesaurus*. These grooves are absent in the strongly-faceted canine of *Thrinaxodon*. The postcanines of *Cynosaurus*, *Platycraniellus*, *Progalesaurus* and *Galesaurus* lack lingual cingula, whereas postcanines in *Thrinaxodon* and *Procynosuchus* display definite lingual cingula and are therefore considered more complex elements.

Phylogeny of basal cynodonts

Updated character scores for *Cynosaurus suppostus* were included in the data matrix provided by Kammerer (2016), who analysed basal cynodont interrelationships. Kammerer (2016) used the matrix provided by Botha *et al.* (2007) as the basis for his revised analysis. This originally included 59 craniodental characters scored for one gorgonopsian, six therocephalians and 10 non-mammaliaform cynodonts, but Kammerer (2016) eliminated five therocephalian taxa from the analysis. We retained the gorgonopsian *Cyonosaurus* and the basal therocephalian *Lycosuchus* as outgroups and added *Platycraniellus* to the ingroup. The taxon reduction in the data matrix as presented by Kammerer (2016) resulted in the deletion of some characters, as they showed no variation in the taxa represented in the revised matrix. Therefore characters 10 (boss/crest anterior to the interpterygoid vacuity), 11 (suborbital vacuity in the palate), 16 (postorbital bar), 18 (temporal fossa), 23 (occipital crests), 34 (stapes), 36 (mastoid and quadrate processes of the paroccipital process), 41 (longitudinal depression on the lateral side of the dentary), 53 (lower canine) and 57 (postcanine occlusion) were deleted (see Supplementary information 1).

We also introduced other changes in the data matrix. For character 4, incisive foramen; absent (0), present and closed posteriorly (1), we added a new character state: present, not closed posteriorly (2) and rescored all taxa. The following changes were made to the scores of *Cynosaurus* (scoring of characters of the lower jaw should be considered with caution as we could only check the condition in the juvenile BP/1/4469): character 14, pineal foramen we changed from present (0) to absent in adults (1), based on Benoit *et al.* (2015); character 25, paroccipital process in the base of the posttemporal fossa, was rescored from '?' to present (0); character 40, angular region of the dentary, was rescored to anterior to the postorbital bar (0) (but the angle of the dentary is not totally preserved in BP/1/4469); character 43, foramen on external surface of the lower jaw between dentary and angular, changed from '?' to absent (0); character 46, position of the dentary/surangular dorsal contact, changed from closer to postorbital bar (0) to midway (1); character 49, lower incisor number, changed from '?' to three (1); character 53, lower canine, changed from '?' to large (0), based on AM4947; character 40, angular relation of the dentary, changed from at the same level or posterior (1) to anterior to the postorbital bar (0); character 30, pterygo-paroccipital foramen, changed from present (1) to '?'.

Some changes were also made to character scores for other taxa. For *Abdalodon*: character 9, interpterygoid vacuity in adults, changed from '?' to present (0) as originally stated by Botha-Brink and Abdala (2008) after further preparation of the specimen (F.A., pers. obs.); character 47, upper postcanine morphology, changed from '?' to sectorial with lingual cingulum (3), as this morphology is visible on the right side of *Abdalodon* (Botha-Brink & Abdala 2008). For *Dvinia*, character 28, epipterygoid ascending process, changed from '?' to greatly expanded (2), after Ivakhnenko (2013).

We reinstated the character state for character 45: masseteric fossa in the dentary, notch in the base of the coronoid process (1) and scored it in *Charassognathus*. Considering its placement on the dentary, our primary homology hypothesis is that the notch represents a precursor of the masseteric fossa. Masseteric or masseteric-like fossae have been described at least in two therocephalians, the akidnognathid *Olivierosuchus* and the bauriid *Microgomphodon* (Botha-Brink & Modesto 2011; Abdala *et al.* 2014) and also seems to be present in *Promoschorhynchus* (F.A., pers. obs.). However, there is no evidence in therocephalians of the presence of a notch as in the dentary of *Charassognathus*. We assume this notch is correlated with occlusal muscles based on its position high in the coronoid process, coincident with the placement of the masseter process in three late Permian cynodonts: *Procynosuchus*, *Dvinia* and *Abdalodon*. We rescored this character in *Galesaurus* and *Progalesaurus* from absent (0) to fossa extends to the angle of the dentary (2). Kammerer interpreted the fossa as present only if there is a ridge clearly delimiting this structure anteriorly (C. Kammerer pers. comm.). Here, we reworded this character based on homology of the attachment area of the masseter muscle (which would be located on the angle of the dentary even if the ridge limiting the fossa is not

present). Our interpretation of the presence of this muscle in *Galesaurus* and *Progalesaurus* implies its insertion on the area of the angle of the dentary (see Jasinoski & Abdala 2017 and Lautenschlager *et al.* 2016).

For *Charassognathus* we changed character 60, diastema between maxillary canine and postcanine, from present (1) to absent (0), as the gap between the teeth is small, unlike the large diastema observed (and diagnostic) in *Abdalodon*. Multistate characters 1, 4, 6, 8, 15, 18, 23, 32, and 36–38 were treated as additive considering adjacency of character states (Lipscomb 1992).

The program TNT (Tree Analysis Using New Technology) version 1.5 was used for searching for most parsimonious trees (Goloboff *et al.* 2008; Goloboff & Catalano 2016). Considering the size of the data matrix (52 characters and 14 taxa) an implicit enumeration was used for the search of shortest trees. We also present Bremer Support and bootstrapping (Fig. 11).

The analyses resulted in 16 most parsimonious trees (mpt) of 108 steps, with the majority rule consensus depicted in Fig. 11. Bremer support values higher than 1 are recovered for Cynodontia, Epicynodontia, Galesauridae and Eucynodontia (Fig. 11).

We recovered a successive series of polytomies, the basal one recovering the monophyletic groups Charassognathidae, including *Charassognathus* and *Abdalodon*, as proposed by Kammerer (2016); Procynosuchia, formed by the cosmopolitan *Procynosuchus* and the Russian *Dvinia*; and *Cynosaurus* + Epicynodontia. Procynosuchia was originally proposed by Kemp (1982), but also included galesaurids (*Galesaurus* was later employed by Hopson & Kitching (2001) to define Epicynodontia and thus excluded from the 'procynosuchian' grade). More recently, Kemp (2005) used Procynosuchia to include the same taxa included here, but he considered the group paraphyletic. Resampling and Bremer support for Charassognathidae are poor (Boostrap value of 45 and Bremer support of 1) and extremely poor in the case of Procynosuchia, as the group is only recovered in the majority consensus tree (Bootrap value of 3). Kammerer (2016) considered Charassognathidae as well supported, citing the boostrap value of 84. However the Bremer support for the group was 1 (Kammerer 2016: fig, 6), indicating poor support for this clade.

The second polytomy in our analysis corresponds to Epicynodontia, including *Cynosaurus*, Galesauridae (formed by *Progalesaurus* and *Galesaurus*) and a group including remaining cynodonts (Fig. 11). Six synapomorphies support Epicynodontia: character 1, short septomaxillary facial process (1); character 14, moderately deep zygomatic arch dorsoventral height (1); character 31, incipient lateral crest of the dentary (1); character 36, masseteric attachment area on dentary, extends to angle (3); character 37, dentary-surangular dorsal contact, midway between the postorbital bar and the craniomandibular joint (1); and character 46, sectorial upper postcanines (1).

Hopson & Kitching (1972) included *Cynosaurus*, *Galesaurus*, *Thrinaxodon*, *Platycraniellus* and *Bolotridon* in Galesauridae (see also Kemp 1982), but this family was later restricted to *Cynosaurus* and *Galesaurus* (Battail 1991) based on the similar palatal morphology of these two taxa. Sidor & Smith (2004) later described a new genus, *Progalesaurus*, which they included in Galesauridae. Our result fails to find unequivocal evidence of *Cynosaurus* as member of Galesauridae (Fig. 11), as the genus is recovered inside the family in only two of the 16 mpt. This is in agreement with phylogenies by Abdala (2007), Botha *et al.* (2007) and Kammerer (2016). Galesauridae in our analysis is supported by two synapomorphies: character 15, presence of a suborbital angulation between maxilla and jugal (1); and character 49, strongly curved main cusp in posterior postcanines (1).

CONCLUSION

Cynosaurus suppostus is a medium-sized late Permian basal cynodont, known from only nine confidently-identified specimens recovered in the Karoo Basin, five of them previously unpublished. Specimens of *Cynosaurus* for which the provenance is known suggest a very restricted geographic distribution of the taxon, within a diameter of approximately 150 kilometres. There are two specimens known from layers of the *Cistecephalus* AZ and six specimens from levels of the *Daptocephalus* AZ

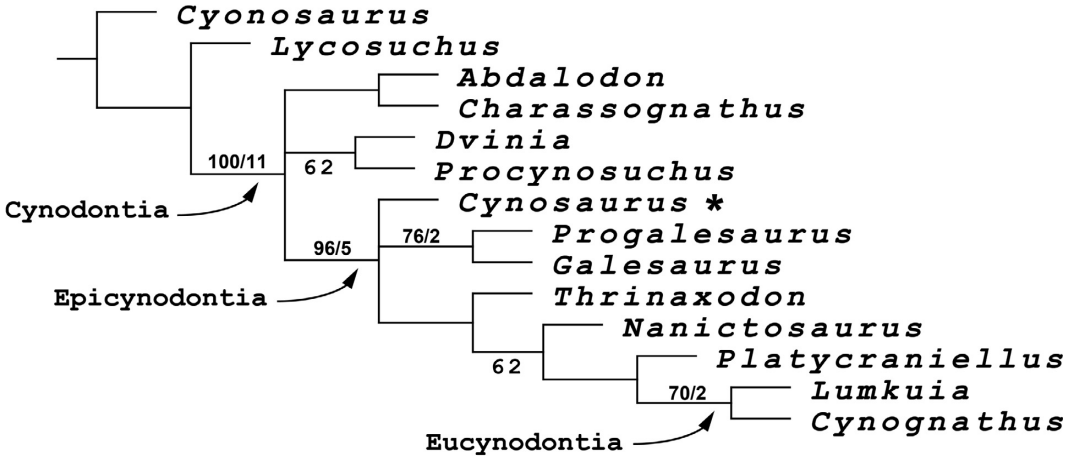


Figure 11. Majority rule consensus of the 16 most parsimonious trees recovered in the phylogenetic analysis of basal cynodonts. Asterisk indicates position of *Cynosaurus*. Numbers below the branch indicate frequency of clades in the fundamental trees. Numbers above the branch represent bootstrapping value/Bremer support (presented only for groups with Bremer support higher than one).

(with one specimen, AM4947, of uncertain provenance).

After a detailed redescription of the skull and dentition, our updated diagnosis reveals three autapomorphies: the subvertical mentum on the lower jaw, robust mandible with a high horizontal ramus, and a relatively broad snout. The adult dental formula is I4/i3, C1/c1, PC 8-9/pc8-9, which has the same postcanine number as the majority of *Galesaurus* specimens and the lower series of *Progalesaurus*. The incomplete secondary palate in *Cynosaurus* similar to that of *Galesaurus* and *Progalesaurus*. The postcanine morphology is a slightly curved main cusp and anterior and posterior accessory cusps; differing from *Galesaurus* (which has a strongly curved main cusp) and from *Progalesaurus* (which shows several additional posterior accessory cusps). Scleral ossicles are preserved in one of the new specimens described, representing only the third instance of a non-mammaliaform cynodont taxon posessing these bones.

An updated phylogeny of basal cynodonts recovered monophyletic Charassognathidae and Probainognathia, but both with poor support. A monophyletic Galesauridae comprises only *Galesaurus* and *Progalesaurus*. *Cynosaurus* is only recovered as a member of this family in two of the 16 mpt, and therefore its identity as a galesaurid cannot be confirmed at present.

ABBREVIATIONS

Institutional

AM	Albany Museum, Grahamstown, South Africa.
MMK	McGregor Museum, Kimberley, South Africa.
AMNH FARB	American Museum of Natural History, Fossil Amphibian, Reptile, and Bird Collection, New York, U.S.A.
BP	Evolutionary Studies Institute, University of the Witwatersrand, Johannesburg, South Africa (formerly the Bernard Price Institute for Palaeontological Research).
BSPG	Bayerische Staatssammulung für Paläontologie und Geologie, Munich, Germany.
NMQR	National Museum, Bloemfontein, South Africa.
NHMUK	The Natural History Museum, London, United Kingdom.
RC	Rubidge Collection, Wellwood, Graaff-Reinet, South Africa.
SAM	Iziko South African Museum, Cape Town, South Africa.
TM	Ditsong National Museum of Natural History (formerly Transvaal Museum, Northern Flagship Institution), Pretoria, South Africa.
UCMP	University of California Museum of Paleontology, Berkeley, U.S.A.

We are indebted to Christian F. Kammerer for significant improvements to the final manuscript. For access to the material studied, we appreciatively thank Sheena Kaal and Roger Smith (SAM), Bernhard Zipfel (ESI) and Billy de Klerk (AM). For additional preparation of specimens BP/1/3926, SAM-PK-K10694, BP/1/4469, and AM4947 we thank Charlton Dube (ESI). Financial support was provided through a National Research Foundation (NRF) student assistant researcher grant under the African Origins Programme of Bruce Rubidge (ESI). We acknowledge and thank Sue Dykes (ESI), Luke Norton (ESI) and Jonah Choiniere (ESI) for advice and assistance with regard to photographic techniques and the use of the drawing software programs of Inkscape and GIMP 2 (GNU Image Manipulation Program). We thank Tea Jashashvili (ESI) for performing micro-computed tomographic scanning of specimens BP/1/3926, SAM-PK-K10694, BP/1/4469, AM4947 and BP/1/1563.

REFERENCES

ABDALA, F. 2007. Redescription of *Platycraniellus elegans* (Therapsida, Cynodontia) from the Lower Triassic of South Africa, and the cladistic relationships of eutheriodonts. *Palaeontology* **50**, 591–618.

ABDALA, F. & SMITH, R.M.H. 2011. Gran hermano en el Pérmico Superior: nuevo cinodonte de Sudáfrica representa la mayor especie del grupo al final del Paleozoico. IV Congreso Latinoamericano de Paleontología de Vertebrados. San Juan, Argentina, 21–24 September 2017.

ABDALA, F. & RIBEIRO, A. M. 2010. Distribution and diversity patterns of Triassic cynodonts (Therapsida, Cynodontia) in Gondwana. *Palaeogeography, Palaeoclimatology, Palaeoecology* **286**, 202–217.

ABDALA, F., HANCOX, P.J. & NEVELING, J. 2005. Cynodonts from the uppermost Burgersdorp Formation, South Africa, and their bearing on the biostratigraphy and correlation of the Triassic *Cynognathus* Assemblage Zone. *Journal of Vertebrate Paleontology* **25**, 192–199.

ABDALA, F., JASHASHVILI, T., RUBIDGE, B.S. & VAN DEN HEEVER, J. 2014. New material of *Microgomphodon oligocynus* (Eutherapsida, Therocephalia) and the taxonomy of southern African Bauriidae. **In**: Kammerer, C.F., Angielczyk, K.D. & Frobisch, J. (eds), *Early Evolutionary History of the Synapsida*, 209–231. Dordrecht, Springer.

ANGIELCZYK, K.D. & SCHMITZ, L. 2014. Nocturnality in synapsids predates the origin of mammals by over 100 million years. *Proceedings of the Royal Society B* **281**.
DOI: 10.1098/rspb.2014.1642

BATTAIL, B. 1991. Les Cynodontes (Reptilia, Therapsida): une phylogénie. *Bulletin du Muséum National d'Histoire Naturelle, 4e Série* **13**, 17–105.

BENOIT, J., ABDALA, F., VAN DEN BRANDT, M.J., MANGER, P.R. & RUBIDGE, B.S. 2015. Physiological implications of the abnormal absence of the parietal foramen in a Late Permian cynodont (Therapsida). *The Science of Nature* **102**, 69.
https://doi.org/10.1007/s00114-015-1321-4

BOTHA, J., ABDALA, F. & SMITH, R. 2007. The oldest cynodont: new clues on the origin and early diversification of the Cynodontia. *Zoological Journal of the Linnean Society* **149**, 477–492.

BOTHA-BRINK, J. & ABDALA, F. 2008. A new cynodont record from the *Tropidostoma* Assemblage Zone of the Beaufort Group: implications for the early evolution of cynodonts in South Africa. *Palaeontologia africana* **43**, 1–6.

BOTHA-BRINK, J. & MODESTO, S. P. 2011. A new skeleton of the therocephalian synapsid *Olivierosuchus parringtoni* from the Lower Triassic Karoo Basin. *Palaeontology* **54**, 591–606.

BRINK, A. S. 1951. Studies of Karroo reptiles: 1. Some small cynodonts. *South African Journal of Science* **47**, 338–342.

BRINK, A. S. 1965. On two new specimens of *Lystrosaurus*-Zone cynodonts. *Palaeontologia africana* **9**, 107–122.

BROOM, R. 1905. On the use of the term Anomodotia. *Records of the Albany Museum* **1**, 266–269.

BROOM, R. 1931. Notices of some new genera and species of Karoo fossil reptiles. *Records of the Albany Museum* **4**, 161–166.

BROOM, R. 1936. On some new genera and species of Karroo fossil reptiles, with notes on some others. *Annals of the Transvaal Museum* **18**, 349–385.

BROOM, R. 1942. Evidence of a new sub-order of mammal-like reptiles. *South African Museums Association Bulletin* **2**, 386.

GOLOBOFF, P., FARRIS, J. & NIXON, K. 2008. TNT, a free program for phylogenetic analysis. *Cladistics* **24**, 774–786.

GOLOBOFF, P. & CATALANO, S. A. 2016. TNT version 1.5, including a full implementation of phylogenetic morphometrics. *Cladistics* **32**, 221–238. DOI: 10.1111/cla.12160

GRAY, J.E. 1862. A synopsis of the species of alligators. *Annals and Magazine of Natural History* **3**, 327–331.

HAUGHTON, S. H. 1918. Investigations in South African fossil reptiles and Amphibia (Part 11). Some new carnivorous Therapsida, with notes upon the brain-case in certain species. *Annals of the South African Museum* **12**, 196–215.

HOPSON, J.A. & KITCHING, J.W. 1972. A revised classification of cynodonts (Reptilia, Therapsida). *Palaeontologia africana* **14**, 71–85.

HOPSON, J.A. & KITCHING, J.W. 2001. A probainognathian cynodont from South Africa and the phylogeny of nonmammalian cynodonts. *Bulletin of the Museum of Comparative Zoology* **156**, 3–35.

IVAKHNENKO, M.F. 2013. Cranial morphology of *Dvinia prima* Amalitzky (Cynodontia, Theromorpha). *Paleontological Journal* **47**, 210–222.

JASINOSKI, S.C. & ABDALA, F. 2017. Cranial ontogeny of the Early Triassic basal cynodont *Galesaurus planiceps*. *The Anatomical Record* **300**, 353–381.

JASINOSKI, S.C., ABDALA, F. & FERNANDEZ, V. 2015. Ontogeny of the Early Triassic cynodont *Thrinaxodon liorhinus* (Therapsida): cranial morphology. *The Anatomical Record* **298**, 1440–1464.

KAMMERER, C.F., ANGIELCZYK, K.D. & FROBISCH, J. 2015. Redescription of the geikiid *Pelanomodon* (Therapsida, Dicynodontia),

with a reconsideration of '*Propelanomodon*'. *Journal of Vertebrate Paleontology* **36**, e1030408.
DOI: 10.1080/02724634.2015.1030408
KAMMERER, C. F. 2016. A new taxon of cynodont from the *Tropidostoma* Assemblage Zone (upper Permian) of South Africa, and the early evolution of Cynodontia. *Papers in Palaeontology* **2** 387–397.
http://dx.doi.org/10.1002/spp2.1046
KAMMERER, C. F. 2017. Rediscovery of the holotype of *Clelandina major* Broom, 1948 (Gorgonopsia: Rubidgeinae) with implications for the identity of this species. *Palaeontologia africana* **52**, 85–88.
http://wiredspace.wits.ac.za/handle/10539/23480
KEMP, T.S. 1979. The primitive cynodont *Procynosuchus*: functional anatomy of the skull and relationships. *Philosophical Transactions of the Royal Society of London. Series B, Biological Sciences* **285**, 73–122.
KEMP, T.S. 1982. *Mammal-like Reptiles and the Origin of Mammals.* New York, Academic Press.
KEMP, T.S. 2005. *The Origin and Evolution of Mammals*. Oxford, Oxford University Press.
KEMP, T.S. 2012. The origin and radiation of therapsids. **In:** Chinsamy-Turan, A (ed.), *Forerunners of Mammals: Radiation – Histology – Biology*, 3–30. Indiana, Indiana University Press.
KITCHING, J.W. 1977. *The Distribution of the Karroo Vertebrate Fauna.* Bernard Price Institute for Palaeontological Research, University of the Witwatersrand, Memoir **1**, 1–131.
LAUTENSCHLAGER, S., GILL, P., LUO, Z-X., FAGAN, M.J. & RAYFIELD, E.J. 2016. Morphological evolution of the mammalian jaw adductor complex. *Biological Reviews* **92**, 1910–1940.
LIPSCOMB, D. 1992. Parsimony, homology and the analysis of multistate characters. *Cladistics* **8**, 45–65.
LIU, J. & OLSEN, P. J. 2010. The phylogenetic relationships of Eucynodontia (Amniota: Synapsida). *Journal of Mammalian Evolution* **17**, 151–176.
https://doi.org/10.1007/s10914-010-9136-8
OWEN, R. 1861. *Palaeontology, or, a Systematic Summary of Extinct Animals and their geological relations.* Edinburgh, Adam and Charles Buck.
OWEN, R. 1876. *Descriptive and Illustrated Catalogue of the Fossil Reptilia of South Africa in the Collection of the British Museum*. London, Printed by order of the Trustees.
SCHMIDT, K. P. 1927 New reptilian generic names. *Copeia* **163**, 58–59.
SIDOR, C.A. & SMITH, R.M.H. 2004. A new galesaurid (Therapsida: Cynodontia) from the Lower Triassic of South Africa. *Palaeontology* **47**, 535–556.
SMITH, R.M.H. & BOTHA-BRINK, J. 2014. Anatomy of a mass extinction: sedimentological and taphonomic evidence for drought-induced die-offs at the Permo-Triassic boundary in the main Karoo Basin, South Africa. *Palaeogeography, Palaeoclimate and Palaeoecology* **447**, 88–91.
VAN HEERDEN, J. 1976. The cranial anatomy of *Nanictosaurus rubidgei* Broom and the classification of the Cynodontia (Reptilia: Therapsida). *Navorsinge van die Nasionale Museum* **3**, 141–164.
VAN HEERDEN, J. & RUBIDGE, B. 1990. The affinities of the early cynodont reptile, *Nanictosaurus. Palaeontologia africana* **27**, 41–44.
VIGLETTI, P.A., SMITH, R.M.H., ANGIELCZYK, K.D., KAMMERER, C.F., FROBISCH, J., RUBIDGE, B.S. 2015. The *Daptocephalus* Assemblage Zone (Lopingian), South Africa: a proposed biostratigraphy based on a new compilation of stratigraphic ranges. *Journal of African Earth Sciences* **113**, 153–164.
https://doi.org/10.1016/j.jafrearsci.2015.10.011